DURABILITY OF CARBON FIBER/VINYLESTER COMPOSITES SUBJECTED TO MARINE ENVIRONMENTS AND ELECTROCHEMICAL INTERACTIONS

by

Md Hasnine

A Thesis Submitted to the Faculty of the

College of Engineering and Computer Science

in Partial Fulfillment of the Requirements for the Degree of

Master of Science

Florida Atlantic University

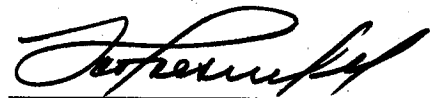Boca Raton, Florida

August, 2010

DURABILITY OF CARBON FIBER/VINYLESTER COMPOSITES SUBJECTED TO MARINE ENVIRONMENTS AND ELECTROCHEMICAL INTERACTIONS
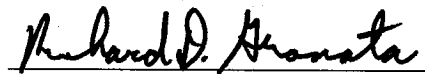
by

Md Hasnine

This thesis was prepared under the direction of the candidate's thesis advisor, Dr. Francisco Presuel-Moreno, Department of Ocean and Mechanical Engineering, and has been approved by the members of his supervisory committee. It was submitted to the faculty of the College of Engineering and Computer Science and was accepted in partial fulfillment of the requirements for the degree of Master of Science.
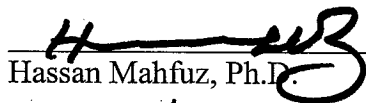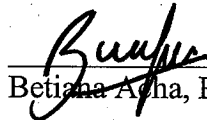
SUPERVISORY COMMITTEE:

Francisco Presuel-Moreno, Ph.D.
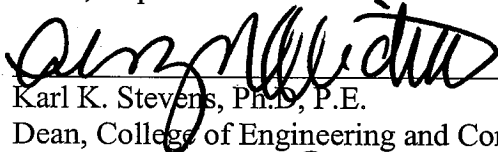Thesis Advisor

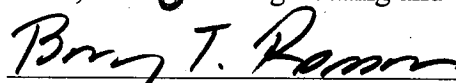Richard Granata, Ph.D.

Hassan Mahfuz, Ph.D.

Betiana Acha, Ph.D.

Mohammad Ilyas, Ph.D.
Chair, Department of Ocean and Mechanical Engineering

Karl K. Stevens, Ph.D., P.E.
Dean, College of Engineering and Computer Science

Barry T. Rosson, Ph.D.
Dean, Graduate College

July 16, 2010
Date

ii

ACKNOWLEDGEMENTS

ABSTRACT

Author: Md Hasnine

Title: Durability of Carbon Fiber/Vinylester Composite Subjected to
                     Marine Environments and Electrochemical Interactions

Institution: Florida Atlantic University

Thesis Advisor: Dr. Francisco Presuel-Moreno

Degree: Master of Science

Year: 2010

Degradation of the Carbon Fiber/Vinylester (CF/VE) polymer matrix composites due to different electrochemical interactions when exposed to seawater or at high temperature had been experimentally investigated. Water uptake behavior of composite specimen was examined based on weight gain measurement. Three point bending test was performed to quantify the mechanical degradation of composite immersed in seawater with different environmental and electrochemical interactions. Finally, Electrochemical Impedance Spectroscopy (EIS) was used to better understanding of the degradation process in CF/VE composite produced by interactions between electrochemical and different environmental conditions. A detailed equivalent circuit analysis by using EIS spectra is also presented in an attempt to elucidate the degradation phenomenon in composites.

DURABILITY OF CARBON FIBER/VINYLESTER COMPOSITE SUBJECTED TO MARINE ENVIRONMENTS AND ELECTROCHEMICAL INTERACTIONS

LIST OF FIGURES

LIST OF TABLES

CHAPTER 1 : INTRODUCTION

1.1   Background

Due to increasing complex design for engineering components and structure, the demand for high performance and weight saving requirements has propelled the engineers and scientists into a continuous search for new materials. After development of the fiber-reinforced plastics, the scope and extent of their application continues to expanding. The term "composite" refers to any material made up of two or more discrete components combined to give better mechanical performance and properties. Polymer composites consist of a stiff and dispersed phase (fiber-reinforcement) that is held together by a continuous polymer phase (matrix) and an interface between fiber and matrix. Therefore, composite materials encompass a wide array of reinforcements and binding materials. Reinforcing materials that are being used include: carbon fibers, glass fibers, aramid fibers whiskers and ceramic particles, as a binding materials epoxy, polyester, vinyl ester, and others are being extensively used. The constituent do not dissolve or merge completely and therefore normally exhibit an interface between one another. Due to this both the reinforcing agents and matrix retain their physical and chemical identities, produce a combination of properties which can not be achieved with either of the constituents alone.

1

Fibers are the principal load carrying members, while the surrounding polymer matrix keeps them in the desired location and orientation. Polymer matrix also acts as a load transfer medium between the fibers, and protects them from environmental degradation due to temperatures, humidity and electrochemical interactions. Therefore, in order for a polymer matrix composite to have superior properties, good interfacial adhesion between fiber and matrix should be achieved. Moreover, the properties of composites depend also on many factors, like the type of reinforcing, volume fraction of reinforcement, chemical additives and orientation of fiber among others.

Fiber reinforced polymer composite materials are widely used in automotive applications, architectural structures and recreational areas like skis, golf clubs and tennis rackets. Moreover, in the last years, polymer composites have gained great interest as structural materials in marine applications specially U.S Navy and offshore, oil industry because of the several advantages over conventional materials like high specific strength, modulus, low weight, good corrosion resistance and excellent damping properties. Composite materials are being used in decks, bulkheads, mast system, propellers, hulls, propeller shaft, rudders, pipes, pumps, valves, machinery and other equipments on large war ship such as frigates, destroyers and aircraft carriers [1].

One of the most famous warships is the Royal Swedish Navy Visby corvette (shown in Fig.1.1) .The hull material is a sandwich structure with carbon fiber/vinylester laminate over a PVC foam core. This material provides high strength and rigidity, low weight, good shock resistance, low radar and magnetic signatures [2]. The U.S Navy is currently developing a new multi-mission destroyer ship, the DDG 1000 Zumwalt class (shown in Fig.1.2), in which the deckhouse will consist of an all composite structure [3].

Figure 1.1: Navy Visby Corvette, Sweden [2]
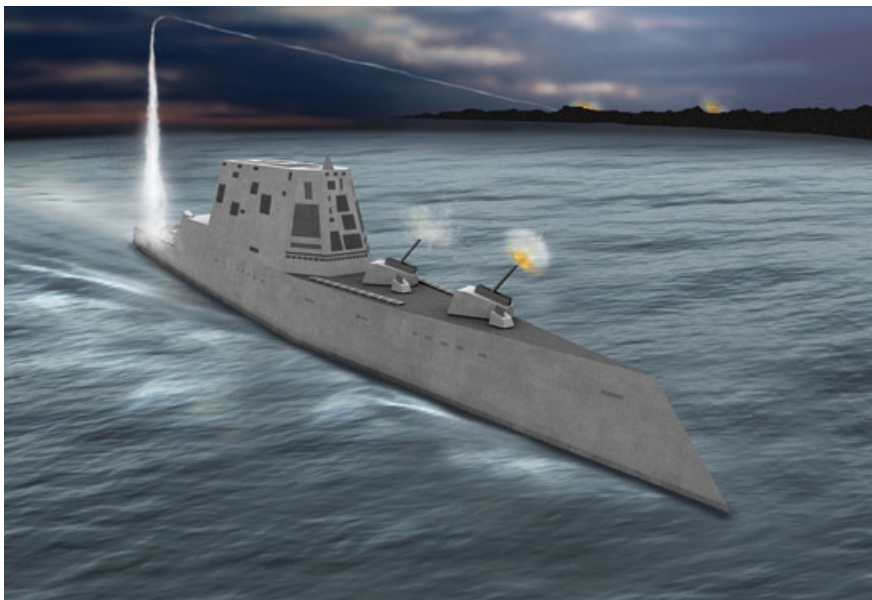
Figure 1.2: U.S Navy DDG1000 Zumwalt multi-mission destroyer [3]

1.2   Fibers for Naval Applications

Fiber is an important constituent in a polymer composite material. A great deal of research has been carried out on the effects of fiber types, fiber volume fraction, architecture and orientation on the fiber reinforced polymer composite. Generally, the fibers occupy 30-70 % of the volume in the composites. The most common type of fibers used in advanced structural applications are glass, aramid and carbon fibers.

In the past the most widely used reinforcement was glass fibers because of their low cost, high tensile strength and impact strength. Glass fiber reinforced polymer composites are often used in marine patrol boat, naval ships, hull casting and masts of submarines. However, the use of glass fiber reinforced composites in marine structures present several disadvantages like their low young modulus because of low stiffness of glass fibers [8] and that glass fibers can be degraded in presence of water [6]. Recently, ships and many marine structures are using carbon fiber composites to overcome the difficulties mentioned above.

Carbon fibers are new breed of high strength materials, which contain 90% of carbon, which have been available since 1940. Carbon fibers have high strength, stiffness and low density. Carbon fibers are chemically inert in most cases and they have excellent thermo physical property and high damping characteristics. Carbon fiber and steeel properties are shown in Table 1.1[5]:

Table 1.1: Comparison of carbon fiber and steel

Materials	Tensile Strength (GPa)	Tensile Modulus (GPa)	Density (g/cm^3)	Specific Strength (Gpa)
Standard carbon fiber	3.5	230.0	1.75	2.00
High tensile steel	1.3	210.0	7.87	0.17

Carbons fibers have superior properties than others common fibers available in market. Typical properties of common fibers used in marine applications are listed in Table 1.2 [7].

Table 1.2: Nominal properties of fibers used in marine applications [7]

Materials	Tensile Strength (GPa)	Tensile Modulus (GPa)	Density (g/cm^3)	Specific Strength (GPa)
Carbon	3.5	230.0	1.75	2.00
Kevlar	3.6	60.0	1.44	2.50
E-glass	3.4	22.0	2.60	1.31

Carbon fibers are used in wide range of applications. Tables 1.3 summarize some of its uses. Carbon fibers can be made from a number of different precursors, including rayon, polyacrylonitrile (PAN) and petroleum pitch. The majority of fibers available today are based on PAN. It dominates nearly 90% of the worldwide sales. The numerous advantages of PAN [$(CH_2CHCN)_n$] fibers are [5]:

➢ Higher melting point (tendency to decompose before melting)

➢ Permits faster rate of pyrolysis without interference of basic structure

➢ High degree of molecular orientation

➢ Larger yield of carbon fiber as polymerized to high temperature

Processing variations lead to three general groups of carbon fibers: high strength (Type I), high modulus (Type II) and ultra-high modulus (Type III) types. Type I, II and III have tensile strength ranges of 3000-6400, 4500-6200 and 2400-4400 MPa and Young's modulus ranges of 235-295, 296-344 and 345-540 GPa, respectively.

Table 1.3: Carbon fiber applications [5]

Uses	Features
Aerospace, road , marine transport and sporting goods	High strength, stiffness and low weight
Missile, aircraft brakes, aerospace antenna and structure, optical benches, large telescope	Low coefficient of thermal expansion, low abrasion and high dimensional stability
Audio equipments, robot arm and pickup arms	High strength and toughness and good vibrating damping
Automobile hood, novel tooling, casing and bases for electronic equipments, brushes	Electrical conductivity
Medical application, surgery and x-ray equipments and bio-materials	Biological inertness and x-ray permeability
Textile machinery	Fatigue resistance and high damping
Chemical industry, nuclear field, valve and seals	Chemical inertness and high corrosion resistance

1.3 Matrix for Naval Application

The resin is another important constituent in composite materials. There are two types of matrices thermoplastics and thermosets. Thermoplastic softer when heated and solidified when cooled in a reversible and repeatable process. Thermoset resins on the other hand, are curable and formed by an irreversible cross-linking between two molecular substances at elevated temperature. This characteristic makes the thermoset resin composite desirable for structural application. These polymers tend to be stronger than thermoplastics and have better dimensional stability, making them a good choice for composites application.

The most common marine polymer matrices used are epoxies, polyester and vinylester. The primary role of the matrix in the composite is i) to transfer stresses between the fibers ii) to provide a barrier against an adverse environment and iii) to protect the surface of the fiber from the abrasion. The mixing of the resin and hardener and the cure temperature play a key role in the cross-linking of the matrix. Matrix is usually post-cured at elevated temperatures to complete the cross-linking reaction. In naval applications, however, the composite sub structural components are typically very large and accelerated post-cure is not feasible. Post-cure may still occur at ambient conditions, but over an extended period of time.

Vinyl ester resin was developed to take the advantage of both the workability of the epoxy resin and fast curing of the polyester. The vinylester has higher physical properties than polyester and costs less than epoxies. Moreover, vinylester resins have fewer ester groups, which make them less susceptible to water degradation by hydrolysis. The small number of ester group means it is less prone to damage by hydrolysis, which

makes them superior in better resistance in water, abrasion and severe mechanical stress offering larger toughness and elongation compare to other resins.

Figure 1.3 shows the chemical structure of a typical vinylester resin.

*denotes reactive sites

Ester groups

n = 1 to 2
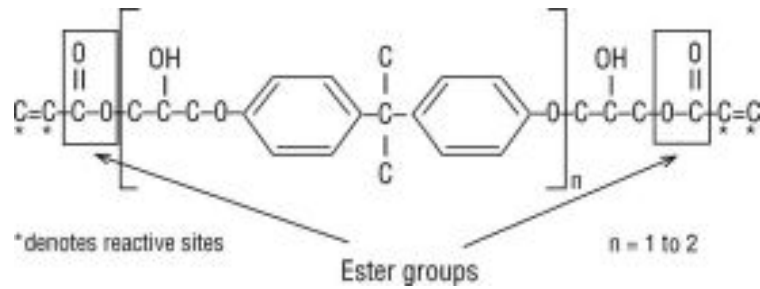
Figure 1.3: Chemical structure of epoxy based vinyl ester resin

As the whole length of the molecular chain is available for absorbing shock loadings this makes vinyl ester resin tougher and more resilient than polyesters. Although they have high chemical and environmental resistance and higher mechanical property than polyester, vinyl ester resin have some drawback like high cure shrinkage, high styrene content and higher cost compared to polyester.

1.4   Environmental factors and electrochemical interactions affecting the polymer matrix composites

During the past 30 years, large numbers of studies have been conducted to investigate the effect of environmental exposure on the physical and mechanical properties of fiber-reinforced composites. Many studies reported on degradation due to erosion, weathering, moisture, fire and temperature. In general, the major environmental factors, which are most detrimental to polymer degradation, are water absorption, temperature, UV radiation and humid air [8-25, 33-41].

It is well known that when composite materials exposed to seawater environment, composites may experience degradation of its mechanical and physical properties. Since, polymer matrix composites absorb moisture from the ambient; the moisture can lead a number of undesirable effects such as degradation of fiber, matrix and fiber/matrix interface. Several studies of durability of composite subject to different environment have been conducted [8, 10, 16, 17, 18, 19].

Temperature has also strong effect on mechanical properties of polymers. When temperature is increased, energy is added to the polymer chains, eventually double bonded carbon atom begins to break and convert into single bond. This leads to cross linking and these cross linking occurs when the polymer is not fully cured. This process embrittles the polymer matrix and lowers the mechanical properties of composite. Large temperature difference also introduces large stresses and leads to microcrack, which increases the water ingress through fiber/matrix interface, reduce the stiffness of the composite and finally contribute to the degradation process.

Another important degradation factor is the exposure to the ultraviolet (UV) radiation. UV radiation is an electromagnetic radiation with wavelength (10-400 nm) shorter than visible light but greater than X-rays' is found in sunlight and they can be emit as electric arc. When ionizing the radiation, it causes the chemical reaction and cause the degradation of materials by photo-degradation. Fiber reinforced composite materials are gaining popularity in outdoor application due to their light weight and high strength. When polymer matrix composites are used in outdoor environment, several elements may be destructive to the polymer and the fiber. While some of the sun's energy radiation is absorbed by the atmosphere, some radiation in the range of 280 to 400 nm reaches the earth surface. This UV radiation can potentially damage the polymeric materials by cleaving the covalent bond and causing embrittleness. Due to absorbing the UV photons, causing the photo oxidation reactions changing the chemical structure of polymer. When composites are exposed in seawater with the simultaneous UV radiation, a more severe degradation of the polymer composite might be possible [12, 13, 14].

Additionally, there are several electrochemical processes that can take place when carbon fiber composites in contact with metal parts are subjected to seawater. One such process is galvanic coupling. Galvanic couple usually refers to two dissimilar metals electrically connected and immersed in a solution. The electrolyte provides a mean for ion transport. Depending on how dissimilar the metals are and the area ratio the galvanic coupling could lead to faster corrosion rate of the anodic metal. Carbon fiber reinforced composite may form a galvanic couple when they are used in conjunction with metals. Carbon fibers are conductive and provide good sites for cathodic reaction to take place (oxygen reduction (ORR) or hydrogen evolution reaction (HER)), but only when solution

reaches the fibers. When a carbon fiber composite is coupled to an alloy, both degradation of the composite and also accelerated the corrosion of the metal is possible. Hence it is important to understand the amount of cathodic reaction that could take place under a polymer film as a function of time. The cathodic reaction at the carbon fiber closest to the surface (and with time even farther in) is likely oxygen reduction reaction (ORR) (at potentials more negative hydrogen evolution reaction (HER) could be the dominant cathodic reaction) which produces hydroxyl ions and could therefore accelerate the degradation of the composite when the hydroxyl concentration is high. The larger the cathode (reaction taking place in the composite) the larger the potential to accelerate the corrosion on the coupled metal, as the anodic and cathodic current need to balance. Equation 1.1 shows the chemical equation for ORR in neutral and alkaline solutions.

$$O_2 + 2H_2O + 4e^- = 4(OH) \qquad (1.1)$$

Carbon fiber composites in marine application are being used to replace conventional metal parts. When a composite is galvanically coupled (electrically connected to other metal) with a metal, it potentially accelerates a corrosion of most metals as carbon fibers are electrically conductive and very noble material. This galvanic interaction between metals and carbon fiber composites could potentially degrade not only the metals but also the composite itself. Tucker and Brown [36] found a blister formation on carbon fiber/vinyl ester composites when they are cathodically polarized by applying -0.9 Vsce potential and exposed them in 3% NaCl solution. They reported that exposed area was 5 cm diameter circular area. The exposure cell allowed water transport from one face only and the cell volume was small allowing relative fast build up of OH⁻ ions. However,

research reported here subjected the samples to full immersion in large seawater tanks. Sloan [34] studied the galvanic degradation of graphite epoxy composite which were suspended in natural seawater and found the causes of degradation under this condition with high pH filling blister cavities.

Stray current corrosion occurs in response to a flow of positive, direct current from a metal into an electrolyte. In case where this current occurs in response to a potential difference other than what exists naturally for the anodic and cathodic processes, is referred to as stray current and the associated deterioration is termed as stray current corrosion. Stray current stimulate corrosion on structure leading to extreme localized attack. Sources [35, 52] of stray current may be electric railways, grounded electric dc power lines, electric welding machines, cathodic protection systems and electroplating plants. Stray currents are those that diverge to other than the intended circuit because they find a parallel and alternative path. Most significant causes of stray current corrosion occur from interference between cathodic protections systems for adjacent structures or in situation where large direct current sources are involved.

Only a few researchers have correlated the strength and durability of composite due to different electrochemical interactions in marine environment [33, 34, 36, 37, 40]. These statements accent the importance of additional studies on the failure and damage mechanism when polymer composites are subjected to both marine environments and electrochemical interactions.

The behavior of composite under service environment is influenced by different factors. One of these is post cure, influencing the composite long-term performance, which needs to be assessed for safe design of composite component. The absorption of

water in polymeric materials is subjected to free volume. The free volume is depends on molecular packing, affected by the cross-link density. Since the water uptake by polymer composite is unavoidable, a proper understanding of the diffusion behavior of non-post cure composite is essential for effective use of polymer composite.

This program is devoted to investigate the durability of composite used in the marine applications. The main goal is to provide the critical information for naval structures design based on a better understanding of environmental and electrochemical degradation of composite materials for such applications.

1.4.1   Moisture absorption in polymer matrix composites

Moisture absorption is a process by which matter is transported from one part of a system to another because of molecular motions. This process is analogous to the transfer of heat by conduction due to random molecular motion. Adolf Fick who first put the diffusion on a quantitative basis by adopting the mathematical equation of heat conduction, first recognized this. The mathematical theory of diffusion is based on the assumption that the rate of transfer of diffusion through a unit area of a section is proportional to the concentration gradient normal to the section. The moisture distributions inside the composite and overall weight gain at any given time are typically modeled by the Fick's second law of diffusion:

$$\frac{\partial c}{\partial t} = D\frac{\partial^2 c}{\partial x^2} \tag{1.2}$$

where C is the moisture concentration, t is the time, D is the diffusivity through the thickness coordinates x.

By assuming the one dimensional problem and flow rate is proportional to the concentration gradient, the solution of the equation is:

$$\frac{M_t}{M_\infty} = 1 - \frac{8}{\pi^2} \Sigma_0^{\infty} (2n+1)^2 \exp\left[\frac{-(2n+1)^2 \pi^2 tD}{h^2}\right]$$ (1.3)

where M_t is the weight gain due to moisture at finite time, M_∞ is the weight gain due to moisture at infinite time and h is the thickness.

In addition, diffusivity can be determined by [24]:

$$D = \pi \left(\frac{h}{4M_m}\right)^2 \left(\frac{M_2 - M_1}{\sqrt{t_2} - \sqrt{t_1}}\right)^2$$ (1.4)

where M_m is the maximum moisture gain in composite after finite time t and M_2 and M_1 are the percent weight gain due to moisture at time t_2 and t_1.

$$\text{Slope} = \frac{M_2 - M_1}{\sqrt{t_2} - \sqrt{t_1}} = \frac{4M_m}{h\sqrt{\pi}}\sqrt{D}$$
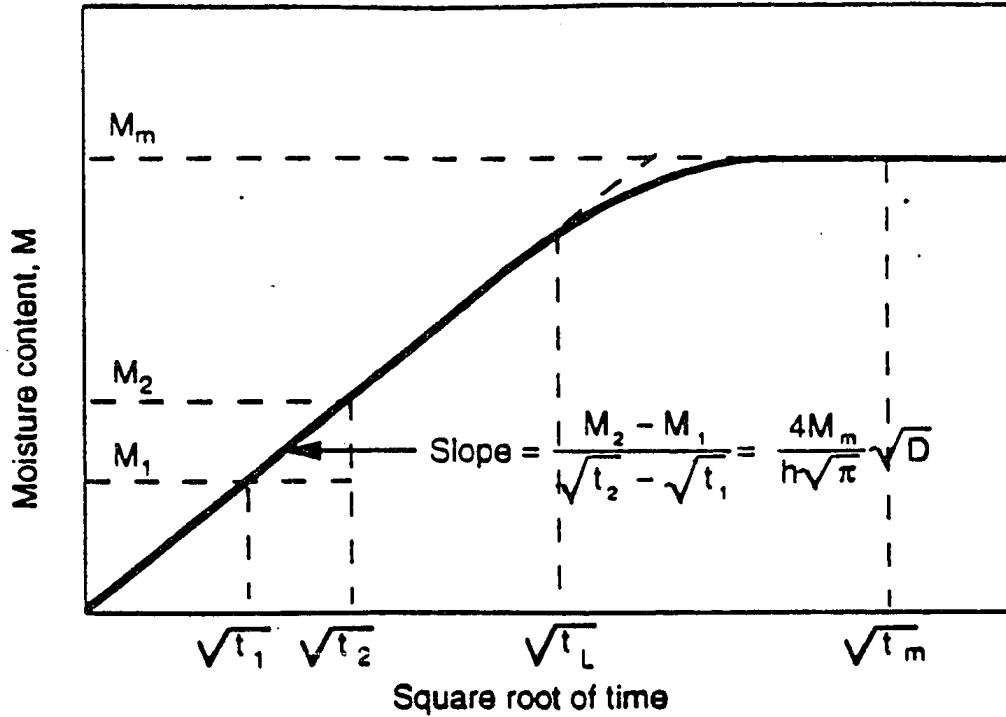
Figure 1.4: Change of moisture content with square root of time [24]

Water absorption in a composites is an enchanting phenomenon that scientists and researchers have been carrying out for long times. Polymer composite's properties might be affected due to water absorption limiting their use in marine environments. Although the primary mechanism for water absorption in composite is concentration gradient Fickian diffusion process is usually dependent on temperature and humidity and it can also affected by others factor [4, 29, 31]. First, water molecule can diffuse through the matrix. The geometry of the diffusion path is also dependent on fiber orientation and the volume fraction of the polymer composite. Secondly, a wicking or capillary flow of water can occur through fiber/matrix interface causing a transport of moisture into the composite. Finally, growth of microcracks or voids, which may be already present at the

15

interface, can provide an easy path for moisture transport into the composite. A blistering formation is a particular example of that.

The rate of diffusion is affected by the temperature and relative humidity [26]. Water diffusion is a thermally activated process. This temperature dependency is represented by Arrehenius relationship as:

$$D = D_0 \, exp\left(-\frac{E_a}{RT}\right) \qquad (1.5)$$

Where, D_0 is a pre-exponential coefficient; R, the universal gas constant (8.3143 J/mol K); T, the absolute temperature (K); and E_a, the activation energy for the diffusion process.

In addition to the aforementioned mechanisms, diffusion rate and water uptake are likely to be affect by electrochemical interactions like galvanic coupling and stray current. Sloan and Talbot [34] mentioned a slight increase in the moisture uptake due to galvanic coupling. However, they found a large scatter of dry weight due to inconsistency of the growing and fall off calcareous deposits.

1.4.2 Environmental degradation of composite materials

Mechanical properties of fiber reinforced polymer composite degrade in terms of mechanical properties when exposed to harsh environment for long periods. A large number of researchers [8-27] have investigated the effects of environmental conditions such as temperature, seawater, UV radiation, humidity and seawater exposure and its combination with electrochemical interactions on the physical and mechanical properties of fiber-reinforced composites.

16

Hammami et al [21] studied the durability and environmental degradation of glass fiber/vinyl ester composite when exposed to seawater and corrosive fluids (nitric acid with different concentration). Long immersion period in seawater and corrosive fluid resulted in decrease in flexural strength values by forming blisters, which may start growing by swelling pressure until final collapse. The combined action of water and corrosive fluid leads to the matrix expansion and pitting may occur. When specimens were immersed in seawater, uncured chemical agents may leach out and leaving the fiber with no protection, which decrease the bonding between fiber and matrix.

Weitsman et al [18] reported effects of fluids on the deformation, strength and durability of polymeric composites. They mentioned that sorption of fluids induces swelling in the polymeric phases, produces residual stress. More significantly, fluids can degrade polymers and fiber/matrix interface by chemical attack (hydrolysis). Reduction of up to 30% in the interfacial strength may occur in Graphite/epoxy systems. Exposure of fluids tends to shorten the fatigue life. Effect of fluids that penetrates the microcrack assists in the reduction of internal toughness, thereby lowering the levels of resistance to fracture. They concluded that fluid enhance the deformation of polymeric composites which must be considered in circumstances where stiffness and deflection are issues of concern.

Gellert et al [17] investigated the effect of seawater on the properties of Graphite fiber reinforced composites. Water uptake behaviors were strongly related to both interface and matrix absorption. Flexural strength fell by 15-21% for the water saturated graphite/polyester and graphite/vinyl ester composites and by 25% for the graphite/phenolic composite.

L.Wu at el [23] characterized the mechanical response of E-glass/Vinyl ester composites immersed in deioinized water, seawater and synthetic seawater. They observed a discernible difference in response between samples immerse in seawater and deionize water, with the former causing a greater level of fiber/matrix de-bonding and outer layer degradation, resulting in increased degradation of the tensile performance and the later causing faster diffusion up to the midplane, resulting in more severe drops in interlaminar shear strength. Drying of specimens even over prolonged periods is not seen to result in complete regain of performance degradation due to sorption processes.

Springer et al. [24, 26] have investigated the effect of temperature and moisture on composite and they found that significant decrease in tensile strength with increase in temperature. They also ascertained that elastic moduli decrease substantially with increase in temperature.

Chin at el [14] characterized the durability of vinyl ester and polyester materials exposed to UV radiation, water, temperature, salt solution and high PH environments. No significant changes were observed in seawater and salt solution at room temperature. The degradation was observed in alkaline and salt solution at 60^0c temperature. However, UV exposure results in surface oxidation as evidenced by the increase in oxygen containing functional groups.

Nakamura et al [12] have studied the effect of environmental degradation using control UV radiation and moisture condensation on flexural failure strength on fiber-reinforced composites. In addition to the exposure condition, materials were subjected to the cyclic loading. A decreasing trend in failure strength was observed for all the exposure conditions with an increase in fatigue loading.

18

1.4.3   Polymer matrix degradation

Moisture diffuses into organic matrix composites leading to change in their mechanical and thermo-physical properties [28]. As the matrix has greater sensitivity to moisture than fiber, matrix dominated properties will be most affected. Moisture diffuses into polymer matrix depends upon a number of molecular and micro structural aspects such as: polarity of the molecular structure, degree of cross linking, degree of crystallinity and presence of residual monomers, hardeners and other water attracting species[28].

Epoxy resin without fiber can absorb water from 2-10% w/w depending upon the base resin and the curing system [29, 30, 31]. Moisture saturation content of vinylester and unsaturated polyester resins are lower than for epoxy resin because of the lower polarity of the ester groups and the aromatic hydrocarbon network.

Polymer can undergo dimensional change due to absorption of water. Resin swelling due to water absorption has a significant impact in the performance of composites. Initially, water is absorbed by a diffusion process into the free volume spaces of the resin. Water is attracted by polar functional groups of heavily cross-linked epoxy and polyester resin molecules, the amount of water getting into the resin exceeds the amount of free volume spaces available, which leads to swelling of the resin [31]. As a result, the hydrogen bonds between polymer molecules are broken. This is known as plasticization and it leads to the fiber/matrix de-bonding. Due to non-uniformity of the moisture in the composite, matrix swelling is also non-uniform and these develop differential stress. Because of differential stresses, fiber/matrix de-bonding can be severe for glass and carbon fiber composites, where fibers are rigid.

Vanlandingham et al [29] have studied moisture induced swelling of Epon 828 epoxy resin with amine curing agent and reduction of glass transition temperature. They reported a relation between moisture induced and its swelling strain. Moisture induced swelling strains increased with increasing moisture content. They also reported the reduction in glass transition temperature due to moisture absorption. Glass transition temperatures were reduced in the range of 5-20^{0}C and were larger for amine rich samples than for epoxy rich samples.

1.4.4 Electrochemical degradation of composites

To fully utilize carbon fiber a composite in naval structures, the state of galvanic coupling is required to be analyzed. Alias et al [33] performed a galvanic coupling test on carbon fiber/vinyl ester composite coupled with aluminum and/or steel and exposed them to 3.5% NaCl solution for 720 hours. They concluded that composite degraded either forming a blister or dissolution of polymer. They did not found any damage for open circuit conditions after 90 hrs. By applying negative -0.65 and -1.2 potential, damage of the composite surface was observed by scanning electron microscopy. Another study [33] found that shear strength decreased due to galvanic coupling of carbon fiber composite with aluminum/steel.

Bellucci et al. [37] have studied the galvanic corrosion of composites under different temperature and fully immersed the specimens into 3.5% NaCl solution. They found that galvanic corrosion of aluminum alloys increased with increase of the temperature. The same author [40] investigated the effect of cathodic to anodic area ratio on the galvanic corrosion induced by graphite epoxy composite materials. It was

observed that galvanic corrosion of aluminum alloys couple with graphite epoxy composite is linearly dependent on the cathodic to anodic area ratio while galvanic corrosion observed by coupling with stainless steel is less severe.

1.5   Electrochemical impedance spectroscopy

To characterize the durability and performance of the many engineering material subjected to different environmental condition, material science has developed different techniques, most of them destructive in nature. In the last few decades, non-destructive methods have been developed as an alternative.

Electrochemical impedance spectroscopy (EIS) is one of these non-destructive techniques. EIS is a powerful method to characterize the electrical properties of materials and their interfaces with electronically conducting materials. EIS is of particular interest as a research tool that can be used to characterize the degradation processes that takes place when materials immersed seawater or exposed to other aggressive environments. EIS is used to identify and estimate the kinetic and mechanistic information. EIS is being used in a variety of fields e.g. corrosion, water uptake, semiconductors, batteries, electroplating and electro-organic synthesis [54]. Electrochemical techniques have been used extensively in the study of corrosion phenomena, both to determine the corrosion rate and to define degradation mechanisms.

EIS technique applies a small amplitude (10 to 20 mV peak to peak) sinusoidal signal at multiple frequencies. By applying the sinusoidal potential signal to an electrochemical

cell, electrochemical impedance is measured by measuring the output current and potential through the cell.

The applied sinusoidal signal is given by[51]:

$$E = E_0 \sin(\omega t) \tag{1.6}$$

where E_0 is the amplitude of the signal and ω is the radial frequency, $\omega = 2\pi f$; $f =$ frequency

The output signal can be expressed as:

$$I = I_0 \sin(\omega t + \phi) \tag{1.7}$$

where I_0 is the amplitude and ϕ is the phase angle.

The impedance can be defined as:

$$Z(\omega) = \frac{E(t)}{I(t)} \tag{1.8}$$

Its modulus of the impedances is $|Z(\omega)| = \dfrac{E_m}{I_m}(\omega)$ and phase angle is $\theta(\omega)$. The impedance of an electrochemical interface can be expressed as a complex number that can be either in polar coordinates or in Cartesian coordinates. In cartesian coordinate, impedance can be written as : Z (ω)= ReZ+jImz where ReZ and ImZ are the real part and imaginary part of the impedance. The relationships between the quantities are:

$$|Z|^2 = (\operatorname{Re} Z)^2 + (\operatorname{Im} Z)^2 \text{ and}$$

$$\theta = Arc\tan\left(\operatorname{Im} Z \middle/ \operatorname{Re} Z\right), \text{ Re (Z)} = |Z|\cos\theta \text{ and Im (Z)} = |Z|\sin\theta$$

The impedance observed in the system can be break down into equivalent circuit elements. The common circuit elements consist of resistor, inductor and capacitor. A list of basic circuit element, their equation and impedance calculation can be shown in Table 1.4.

Table 1.4: Common Circuit elements used in the model [45]

Component	Impedance
Resistor(R)	$Z=R$
Inductor(L)	$Z=j\omega L$
Capacitor(C)	$Z=\dfrac{1}{j\omega C}$
Warburg(W)	$1 \Big/ Y_0\sqrt{(j\omega)}$
Q(CPE)	$1 \Big/ Y_0(j\omega)^{\alpha}$

EIS spectra can be plotted in various forms. The most common of which are Nyquist and Bode plots. By plotting the data in these forms, some insight into the basic circuit element constituting the physical processes may be gained. EIS data is commonly analyzed by fitting to an equivalent electrical circuit model that attempts to describe the electrochemical processes, which are taking place in the system. The fitting to the models allows to estimate the electrochemical parameters of the system e.g., the double layer capacitance, coating capacitance, polarization resistance or charge transfer resistance. The model is fitted with software that performs a least square fitting operation [45] that adjusts the values for the various model parameters.

1.5.1   Application of EIS to polymer matrix composites

Researchers have been using EIS as a tool to understand and identify how the degradation of composite materials due to exposure in seawater with different electrochemical processes [33, 34, 36, 37, 39].

J.Qin et al. [42] studied an impedance test on carbon fiber composite under open circuit condition. They found that impedance decreases with exposure time. One possible mechanism they mentioned for decrease of impedance under open circuit condition is the moisture absorption either by diffusion of transport through the pre-existing defects in the polymer matrix.

Kaushik, et al. [39] employed the EIS on carbon fiber/vinyl ester composites to evaluate the damage when composites are subjected to 3.5% NaCl solution. They concluded that EIS could be applicable to examine the degradation of carbon fiber composite by electrochemical processes. In Kaushik, et al [39] experiment, composites were subjected to two electrochemical processes a) open circuit potential and b)cathodically applied negative potential -0.65 $V_{(SCE)}$ and -1.20 $V_{(SCE)}$ and impedance measurements were performed as a function of time. The impedance spectra results from electrochemical processes were compared with the results from the impedance data for unexposed specimens. It was found that cathodically polarized composites have lower pore resistance (Rpo) than the pore resistance of open circuit potential specimens. As observed in figure 1.6, Kaushik noticed that Rpo for cathodically polarized composite decreased with time but remained constant for specimens at open circuit potential. This suggests that there is additional composite degradation when cathodically polarized and

exposed in aqueous solution. Kaushik also proposed the model shown in figure 1.5 to interpret their EIS results.
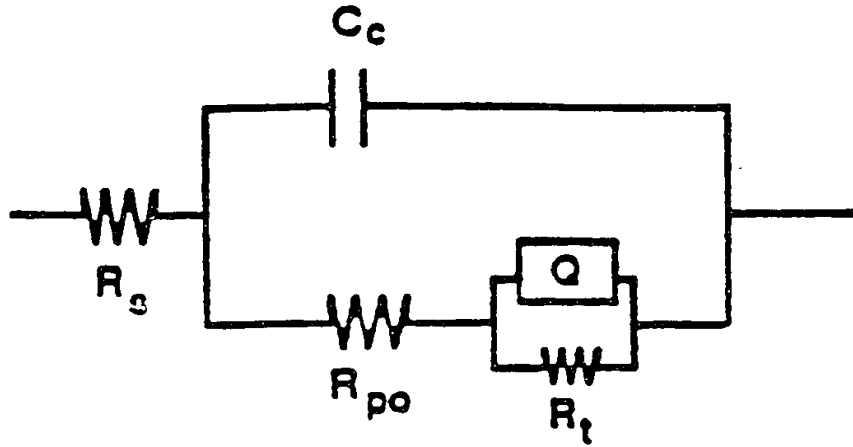
Figure 1.5: Equivalent circuit used to fit impedance data for the carbon
Fiber/vinylester composite [39]
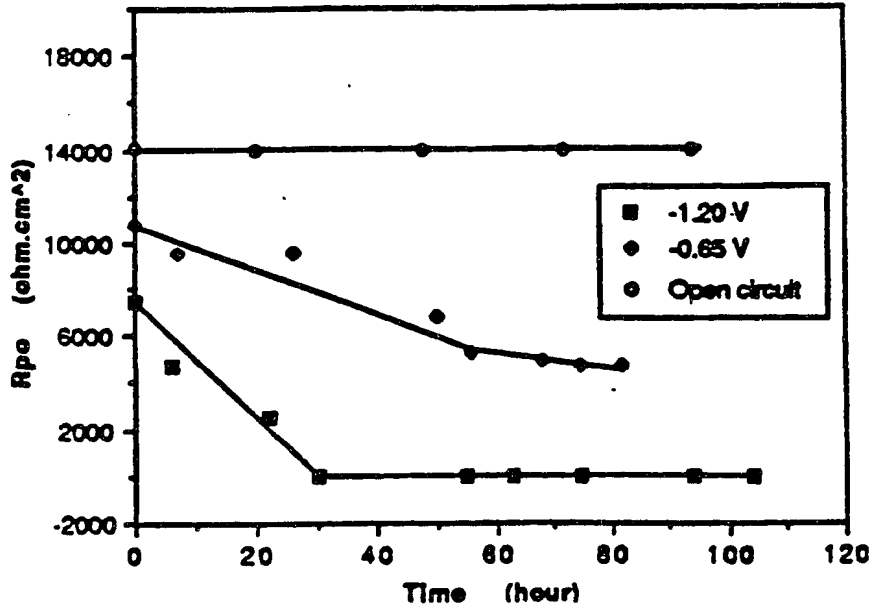
Figure 1.6: Plot of pore resistance as function of time [39]

Alias and Brown [33] has also used the EIS to evaluate the degradation of composite due to galvanic coupling. Alias and Brown [33] propose two mechanisms for degradation of composite in marine environment. One possible mechanism is polymer dissolution of the polymer covering the carbon fibers closest to the surface and causes loss of matrix material. Alias also, found that polymer dissolution is potential dependent i.e, polymer dissolution decreasing with time at -0.65 V_{SCE} while rapid at -1.2 V_{SCE}. The second mechanism is blister formation due to local pH increase resulting from OH- build up because of a greater cathodic reaction. They also included the additional factors such as strength of polymer, diffusion rate and location of the species forming an osmotic pressure affect the degradation of composite.

F.Bellucci [40] found that galvanic corrosion of aluminum and steel when they are coupled with carbon fiber reinforced composite depend on the cathode to anode area ratio. They used the composite as a cathode and observed the vigorous corrosion effect on aluminum compared to steel. That is why they have discouraged the aluminum alloy in coupling with carbon fiber composite due to high galvanic currents. In other study, Bellucci[37] investigated the effect of metal and temperature on galvanic corrosion when coupling with carbon fiber composite. They noticed that galvanic current increases with increase of temperature.

The impedance response of a coating and the matrix of a composite are similar because both are built from polymer systems. Coatings and carbon fiber composites absorb water and degrade when exposed to aqueous environment. In addition, what makes the comparison interesting is the similarity in the physical meaning in both systems. For example, capacitance associated with the coating may be analogous to the

26

capacitance due to matrix material of the composite. Similarly, decreasing pore resistance in a deteriorating coating system is analogous to the reduction in pore resistance with exposure time that is associated with defective matrix composites immersed in seawater. Composite can be visualized as a system made up of many microelectrodes, where carbon fiber can act as discrete conductors. Hence, many electrodes are present each contributing to the total impedance of the system. In addition, each of the electrodes has its own electrochemically active area. The matrix that surrounds the fiber may be not perfect and might typically behave as a coating, although in a more complex way. This means each of these electrodes has its own equivalent electrical analogue, which could be represented as transmission line-like behavior [38].

The capacitance of a coated substrate changes as it absorb water because water have high dielectric constant. In addition, EIS can be used to measure that change. Coating response to EIS can provide information regarding dielectric properties and coating capacitance. At low frequency, EIS can provide information about coating resistance, corrosion reaction at the metal coating interface as a direct result of water uptake and diffusion of the electro active species thorough the surface film on the electrode. Relatively, high frequencies can provide information about the properties of coating and its changes during the exposure to the electrolytes. A similar mechanism is likely to take place on CF/VE composites. Hence, EIS can be also used to monitor water uptake on CF/VE composites, although the water uptake is more complex on composites materials.

Kendig and Schully at el [41] reported that water uptake leads to an increase in the dielectric constant of the coating. This increase is quite sensitive to the water uptake

because the dielectric constant of water phase is twenty times that for the coating. The volume percentage of absorbed water can be obtained from the following equation:

$$\varepsilon(t)\Big/\varepsilon(0) = C_c(t)\Big/C_c(0) = 80^V \qquad (1.9)$$

where $C_c(0)$ is the initial coating capacitance, V is the volume percentage of absorbed water.

Vinci et al [32] used the EIS to determine the volume percentage of absorbed water at the composite interface. After 81 days of hygrothermal exposure, EIS spectra revealed that the percent volume uptake of water at the interface was 12.4% and 27.5% for CF/VE8084 and CF/VE510 composites respectively.

1.6 Research Outline

Durability of composites is one of the properties studied when considering new composite materials for naval structural application. This project is devoted to understand and identify possible degradation mechanisms due to different electrochemical interactions when carbon fiber/vinylester (CF/VE) composites are exposed to seawater or at high humidity environment.

The main goals of this project are:

1.) Investigate if stray currents might accelerate CF/VE composite degradation.

2.) Investigate how galvanic couples between alloys and CF/VE composites of interest might accentuate the degradation of the CF/VE composite.

3.) Investigate UV degradation of polymeric component of a CF/VE composite

Water uptake behavior of composite specimen is examined based on weight gain measurement. Three point bending test is performed to quantify the mechanical degradation of composite immerse in seawater with different environmental and electrochemical interactions. Finally, EIS is used to better understanding of the degradation process in CF/VE composite produced by interactions between electrochemical and different environmental conditions.

CHAPTER 2 : EXPERIMENTAL METHOLOGY

This chapter describes the experimental program, which is designed to achieve the purpose of this research. This includes fabrication of materials, specimen preparation, exposure periods and different test conducted.

Gravimetric and mechanical testing are conducted to identify the degradation processes. Electrochemical Impedance Spectroscopy is performed as a non-destructive technique to better understanding of the degradation processes that could results from different electrochemical interaction in marine environment on carbon fiber/vinyl ester composites.

2.1 Materials and Specimens

2.1.1 Materials

In this project, T700 carbon fiber with FOE sizing (supplied by Toray Inc) is used as fiber reinforcement. The specifications of the T700 carbon fibers (given by manufacturer) are listed in Table 2.1.

Table 2.1: Manufacturers specifications for carbon fiber T700

Specifications	T700 carbon fiber
Tensile strength (GPa)	4900
Modulus (GPa)	230
Strain to failure (%)	2.1
Density (g/cm^3)	1.8

Two types of vinylester resins are used; Derakane 8084 (VE8084) and Derakane 510A-40 (VE510A) supplied by Ashland. Specifications of the vinyl ester resins provided by the manufacturer are listed in Table 2.2.

Table 2.2: Manufacturers specifications of matrix materials

Specifications	VE8084	VE510A
Density (g/mL)	1.02	1.23
Dynamic viscosity(mPa.s)	360	400
Styrene content (%)	40	38
Tensile strength (Gpa)	76	86
Tensile Modulus (Gpa)	2.9	3.40
Flexural Strength (Gpa)	130	150
Flexural Modulus (Gpa)	3.3	3.6

Unidirectional composites, consisting of 6-8 plies, are made from T700/VE8084 and T700/VE510A using vacuum assisted resin transfer molding (VARTM) at room temperature (RT). The VARTM method is recognized by the U.S Navy as a low-cost process for the fabrication of high performance composite ship structures. All composite panels were fabricated using VARTM technique at FAU T-11 lab, Boca Raton.

The basic steps employed in the fabrication of composites by the VARTM method are listed:

I. unidirectional carbon fiber ply is laid up on the glass plate previously treated with release agent

II. the preform is covered by a peel ply and distribution layer.

III. the whole dry stack is then vacuum bagged. A full vacuum is drawn to consolidate the panel and inject the resin

IV. resin is allowed to flow into the panel until full wetting occurred.

V. the panel is allowed to cure at room temperature for 24 hours.

The vinylester resin to be infused was formulated to obtain 50-60 min gel time. VE8084 resin was formulated with 1.5 phr of MEKP, 0.18 phr of CoNap 10 %, and 0.05 phr of dimethylaniline (DMA), and VE 510A formulated with 1.0 phr of MEKP, 0.20 phr of CoNap 10 %. For all formulations the VE resin was first mixed with the CoNap and DMA (only for VE 8084) and stirred during 10 minutes and let stand for one hour before adding MEKP. Figure 2.1 illustrates the layout of VARTM technique:
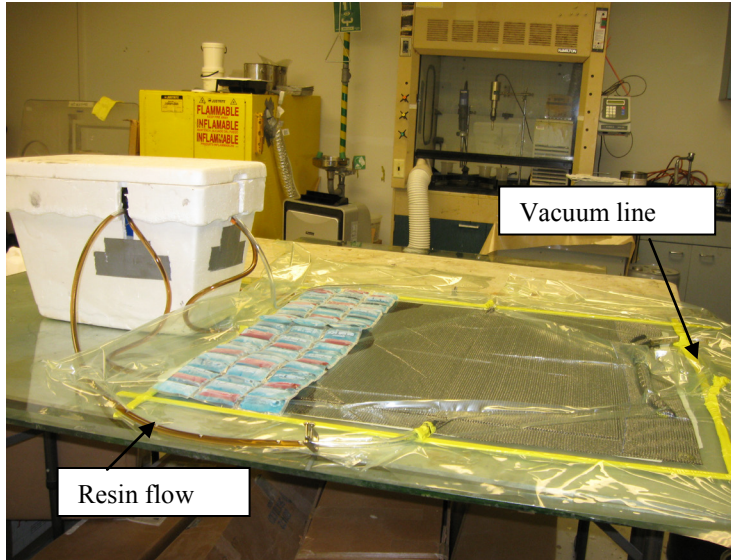
Figure 2.1: VARTM technique layout

Matrix is usually post-cured at elevated temperatures to complete the cross-linking reaction. In naval applications, however, the composite sub structural components are typically very large and accelerated post-cure is not feasible. Post-cure can occur at ambient conditions, but over an extended period of time. The cure and post-cure conditions for VE 8084 and VE 510A are indicated in Table 2.3.

Table 2.3: Cure and Post cure schedule for VE 8084 and VE 510A Composites

Resin	Cure	Post Cure
VE 8084	24 hrs, RT	2 hrs, 99^0C
VE 510A	24 hrs, RT	2 hrs, 120^0C

2.1.2   Test specimens

Unidirectional composite panels made of carbon fiber reinforced vinyl ester resin have an approximate of thickness 1.8 mm. All the test specimens were cut from these panels. The panels were cut by diamond saw with dimensions 100 mm long by 12.7 mm wide for flexure test, 52 mm long by 52 mm wide for gravimetric test and 70 mm long by 70 mm wide for electrochemical impedance test. The specimens and their dimension are shown in table 2.4. Selected specimens were selected for post-cure (See table 2.5). All other samples were stored at laboratory temperature and humidity after cutting for at least 2 weeks before exposure in the different environments took place.

Table 2.4: Specimen dimension for test specimens

Test	Specimen Dimension(mm)
Flexural Test	50.8 x 12.7x 1.85
Gravimetric Test	50 x50 x1.85
Electrochemical Impedance Test	70 x70 x1.85

2.3   EIS specimen

It is well known that carbon fibers are good conductor of electricity. This property was used to apply a conductive paint onto one of edges of the composite (perpendicular to the fiber direction). A small amount of nickel paint was used to form a very thin layer on one fo the two edges perpendicular to the carbon fibers direction. This provided an intermediate media to make a good electrical contact between wire and the specimens, thereby assuring a uniform distribution of current lines inside the composite. A second

layer of nickel paint was applied onto the edges of composite along with wire. The entire

edge was then coated with marine epoxy and let stand for 24 hour for cure at room

temperature. Only the edge with the electrical connection was covered with marine

epoxy. This process was also repeated for flexural specimen subjected to polarization

conditions.

2.3.1 Environmental exposures

Specimens were subjected to different environmental conditions and

electrochemical interactions. Table 2.5 provides the test matrix for environmental

exposures and electrochemical interactions.

Table 2.5: Test matrix for environmental exposures and electrochemical interactions

	No Electrochemical Interaction		Electrochemical Interaction			
	Post Cure	RT-Cure	Stray Current	-0.6V$_{SCE}$	GC-Al-Anode	Zn Anode
SWRT	F,W,E	F,W,E	F,W,E	F,E	F,E	
SW40C	F,W,E	F,W,E	F,W,E	F,E	F,E	
85%RH50C	F,W	F,W				F
SWUV		F,W				

W - Water uptake specimen   50x 50 mm, E - Electrochemical Impedance Spectroscopy (EIS) specimen 70 x 70 mm, F - Flexural strength specimen 12.7 x 50.7 mm

Seawater at Room Temperature (SWRT)

Specimens are immersed in seawater (SW) at room temperature (RT). A large

tank (243 in x 28 in) located in "Center for Marine Material and Corrosion lab at SeaTech

is used to immerse the specimens in this environment. Periodic fresh seawater from the

Atlantic Ocean is circulated in the tank (see figure2.2)
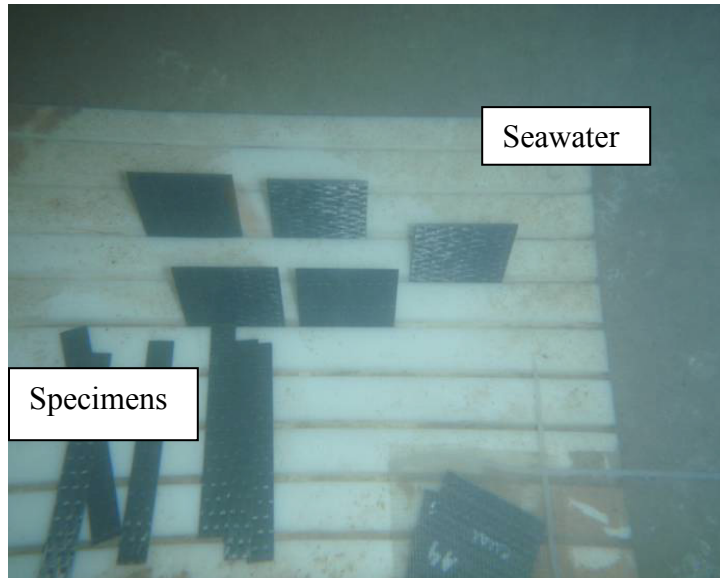
Figure 2.2: Seawater RT exposure

Seawater at 40℃ (SW40C)

Specimens are exposed under seawater at 40℃. A tank (28 in x28 in x21 in) equipped with a heater was used to simulate this environment. The heater is connected to digital temperature controller to maintain the particular temperature. Tank is covered with insulation material to prevent heat loss from the tank and minimize the evaporation. Water was added periodically as needed.

Seawater at RT and UV Radiation (SWUV)

A large fish tank is used to immerse the specimens. In this research, natural exposure, sunlight used as a source of UV rays .The specimens were lift above the water line so that UV can reflect from water. The specimens were also under constant sea-water spray implemented by using a sprinkle system (see figure 2.3)

UV rays
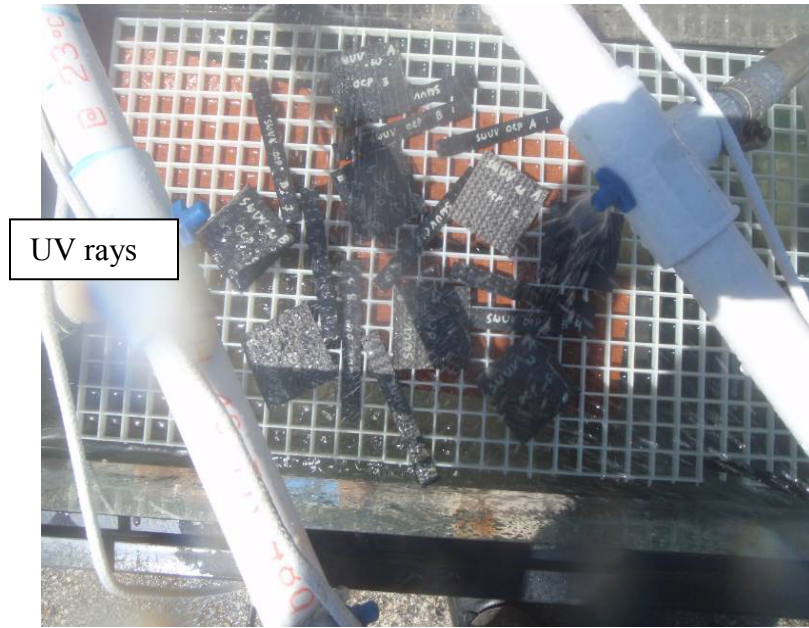
Figure 2.3: Seawater and UV radiation exposure

85 % Relative humidity at 50℃ (85RH50C)

A temperature and humidity control environmental chamber CARON 6030 is used to achieve this condition.

2.4 Electrochemical interactions for samples tested for EIS

Non-polarized or Open Circuit Potential:

The open circuit potential is the potential of the working electrode relative to the reference electrode when there is no potential or current is applied to the specimen. For metal it is also called corrosion potential. Combined with the above-mentioned environmental conditions, specimens are subjected to open circuit condition and then tested for EIS.

Galvanic Coupling:

Selected specimens are polarized by using one of three different set-ups:

a) Samples are coupled to an aluminum anode(see figure 2.4)

b) Samples are cathodically polarized to -0.6V sce by using power supply, a mix metal oxide (MMO) Ti mesh and SCE reference electrode(see figure 2.5)

c) Samples in the 85% RH/50C were coupled with galvanized screw and galvanized wing nuts(see figure 2.6)
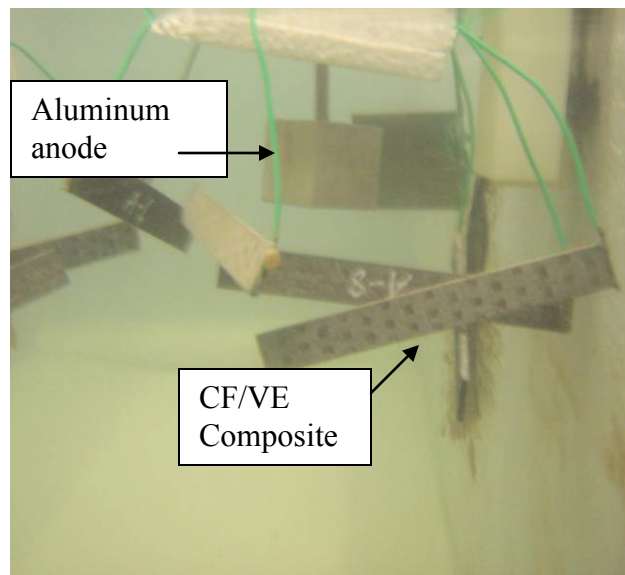
Figure 2.4: Carbon fiber/vinyl ester composite galvanically coupled with Al anode
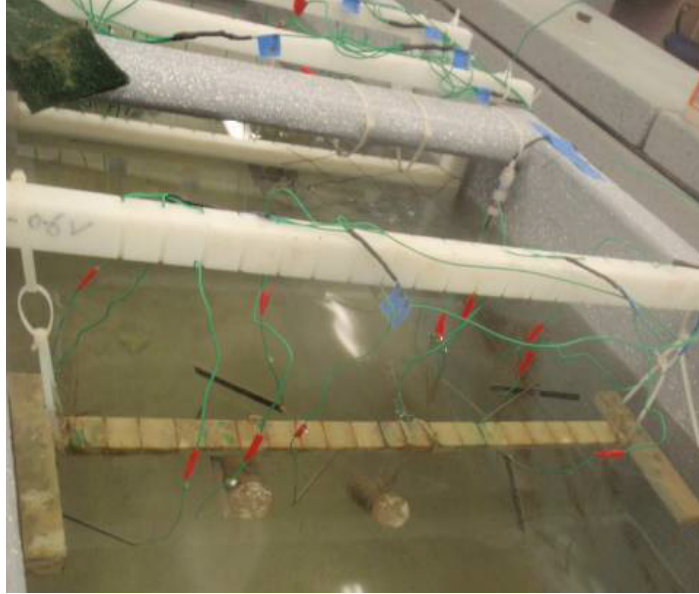
Figure 2.5: Carbon fiber/vinyl ester composite galvanically coupled -0.6V$_{SCE}$ using power supply
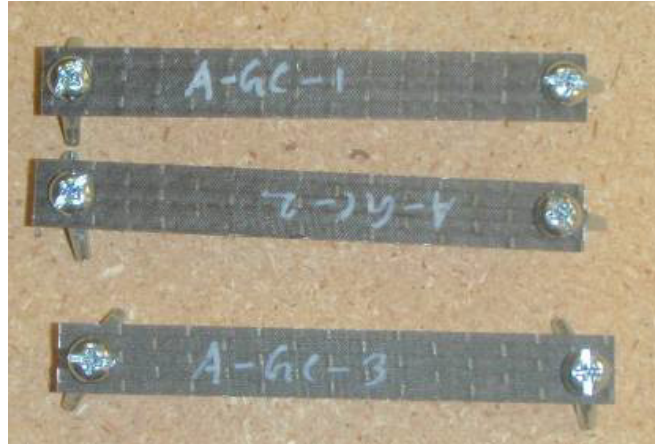
Figure 2.6: Carbon fiber/vinyl ester composite galvanically coupled to Zn screws and wing nuts

Stray Current:

In this research, stray current is investigated as a possible degradation process. The stray current set-up is implemented by placing samples in the path of a sacrificial cathodic protection system. Specimens are placed between the ionic current produced by the cathodic protection systems. CF/VE composites with the edges not sealed were exposed to allow the ionic current to flow through the carbon fibers.

2.5   Gravimetric test

The percentage [43] of moisture gain versus time is monitored for each specimen at a steady state environment, according to ASTM D5229. Specimens were immersed in seawater at different environments (SWRT, SWSC, SW40C, SW40C-SC, SWUV and RH50C). To monitor the water uptake, the specimens are removed periodically, dried carefully with paper towel and weighted in a precision analytical balance (± 0.0001 g). Five replicate specimens are measured under each conditioning.

The moisture absorption was calculated by the following formula:

$$\mathbf{M, \%} = \frac{W_i - W_0}{W_0} \times \mathbf{100} \tag{2.1}$$

where W_i is current specimen weight (g), W_0 represent the weight of the dry specimen (g) and M, % is the percentage of moisture gained.

2.6 Mechanical testing

Three point bending test (ASTM D790) is a simple method to monitor the quality of the structural composite. Flexural tests were done to characterize the degradation of composite under various exposure conditions according to ASTM D 790[44]. The flexural test was performed on a MTS insight 50 machines with 5KN load cell at support span to depth ratio of 16:1 and cross-head speed was calculated by the following formula:

$$R = \frac{ZL^2}{6d} \tag{2.2}$$

where R is the rate of crosshead motion (mm/min), L is the support span (mm), d is the depth of the beam (mm) and Z is the rate of straining of the outer fiber, mm/mm.

Flexural strength and moduli of the composites is calculated by the following formulas:

$$\sigma_f = \frac{3PL}{2bd^2} \tag{2.3}$$

where σ_f is the flexural strength (MPa), P is the load at a given point on the load-deflection curve (N), L is the support span (mm), b is the width of the beam (mm) and d is the depth of the beam (mm).

$$E_B = \frac{L^3 m}{4bd^3} \tag{2.4}$$

where E_B is the modulus of elasticity in bending (GPa) and m is the slope of the tangent to the initial straight line portion of the load-deflection curve (N/mm).
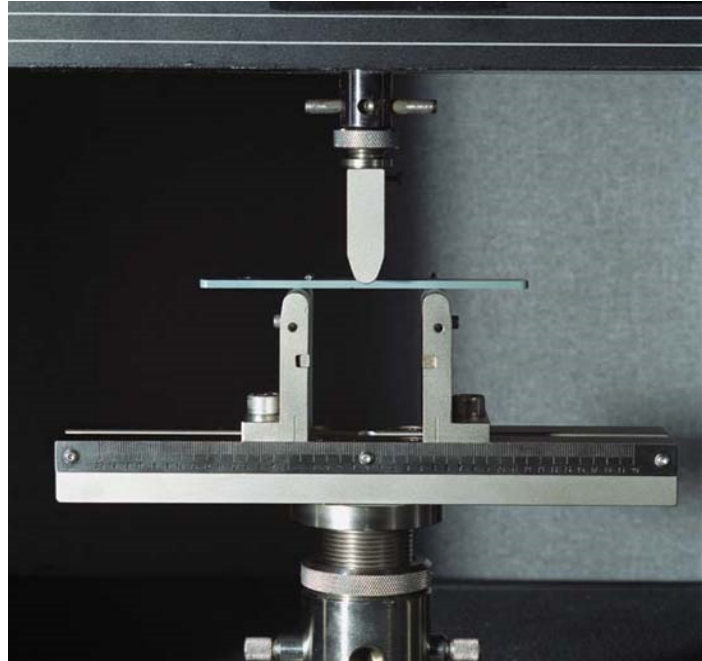
Figure 2.7: Schematic of the flexural testing of composite

2.7 EIS testing

EIS testing was performed on selected specimens after exposure for different amounts of time to the electrochemical and environmental conditions described above. EIS tests were performed on composite specimens at day 0. Initial (day 0) measurements were all conducted starting at room temperature after filling the EIS cell with seawater solution for 20-60 minutes. After this initial EIS test, the specimens were subjected to full immersion in seawater to the specific environments before subsequent EIS tests, removed momentarily to run EIS test and then the specimens were returned to original exposure conditions. The EIS tests were ran in the frequency range of $0.001 - 100,000$ Hz. EIS was typically performed after 1, 5, 14, 32, 63 day of exposure. Impedance

measurements were made using a three-electrode cell configuration. EIS was performed

using a SCE as the reference electrode, a Pt mesh as counter electrode and the composite

specimens was the working electrode. Schematic arrangement is shown in figure 2.8.
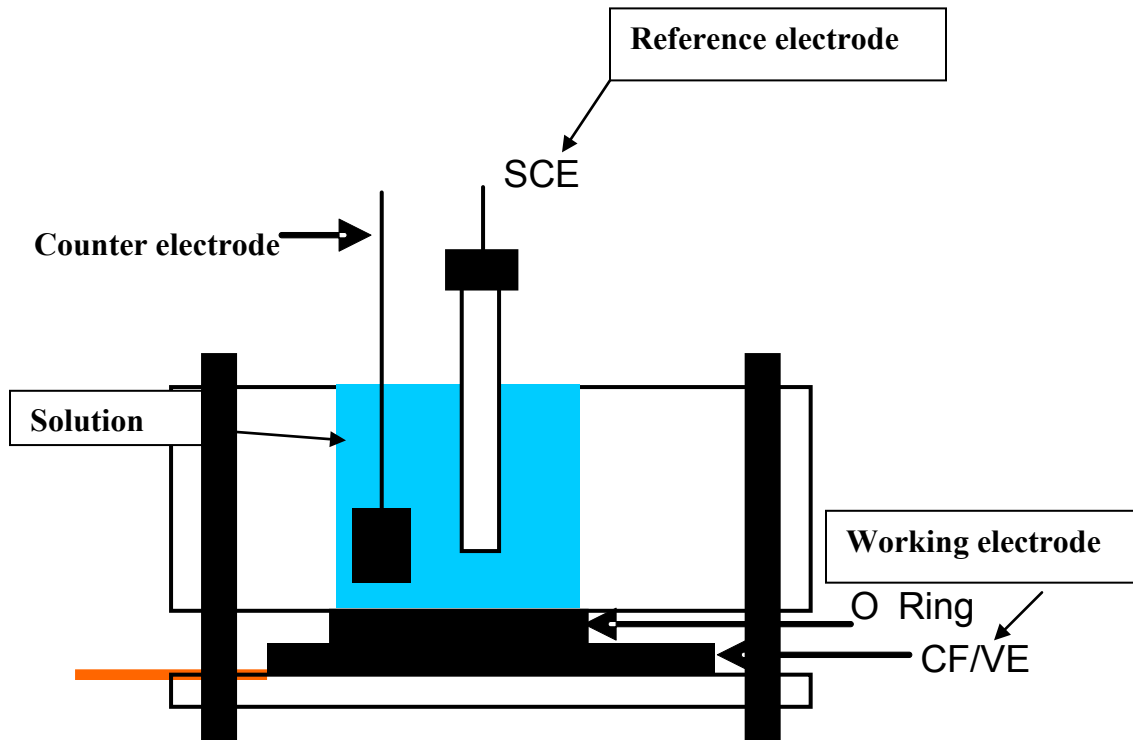
Figure 2.8: Schematic of EIS testing

CHAPTER 3: EXPERIMENTAL RESULTS AND DISCUSSION

3.1   Water Absorption

Figure 3.1 and 3.2 illustrates the weight change vs. square root of immersion time for square (50x50 mm) RT cured carbon fiber/vinylester specimens exposed to seawater (SW) at RT, and 40° C, 85% RH at 50° C and SW at RT and SW at 40° C with stray currents. Similar trend of moisture transport was observed for both resin systems.

As general result, when specimens are immersed in SW, the moisture content increases with time and temperature and higher slopes of the initially linear section of the curve are observed at higher exposure temperatures indicating a higher rate of moisture transport. Exposure to seawater spray and ultraviolet radiation lead to similar moisture absorption behavior than SW at RT exposure. Lower rates of water absorption and moisture saturation content were observed for 50° C and 85% relative humidity (RH) humid air exposure. The presence of stray currents in SW at RT and 40° C do not affect significantly   the   moisture   absorption   for   both   composite   systems

44
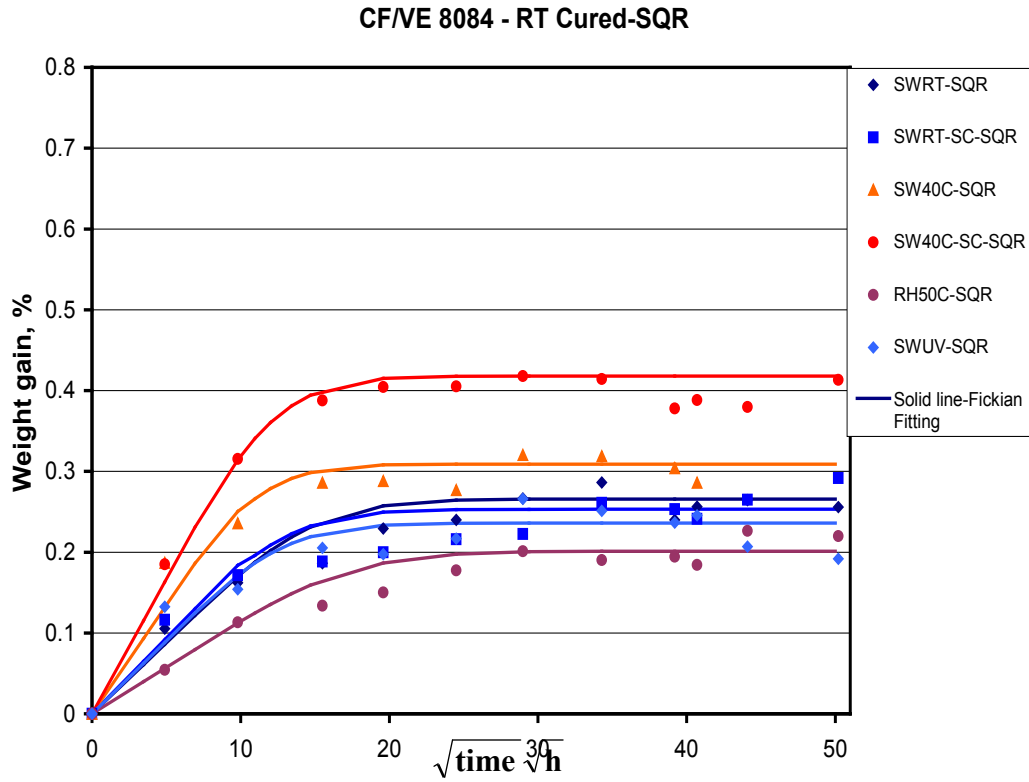
Figure 3.1: Moisture absorption curves for CF/VE8084 RT cured specimens

CF/VE 510A - RT Cured - SQR
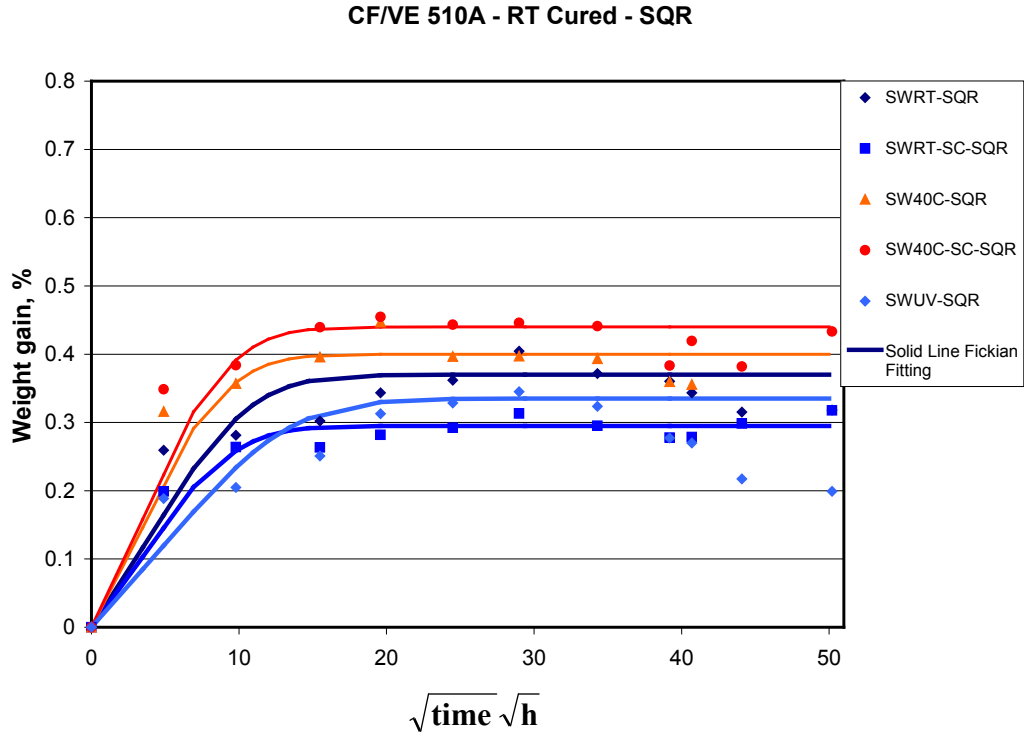
Figure 3.2: Moisture absorption curves for CF/VE510A RT cured specimens

Figures 3.3 and 3.4 depict moisture absorption curves for the flexural RT cured composite specimens exposed to the different environmental conditions.

Similar moisture absorption trends were observed for the flexural specimens over the entire time span investigated. However, CF/VE8084 specimens absorb more water than the CF/ VE510A for all conditioning. This behavior was also observed for the post-cured specimens (see Table 3.2), and this is in good agreement with previous finding by Ramirez et al [52] and Farooq et al [54].

The effect of the geometry on the moisture absorption is still being analyzed. From these set of experiments it can be observed that for CF/VE510A composite the saturation levels for the two geometries are most likely independent of geometry.

Nevertheless, for CF/VE8084 composite, the flexural specimens (100x12.7x1.8 mm) absorb more water than the square ones (50x50x1.8 mm). This finding contradicts the expectations, since the surface areas available for longitudinal diffusion (parallel to the fibers), which commonly dominates moisture diffusion in composites, is smaller for the flexural specimens than for the square ones (1.6% and 3.4%, respectively). Further tests are being pursued to elucidate the reasons for this behavior.
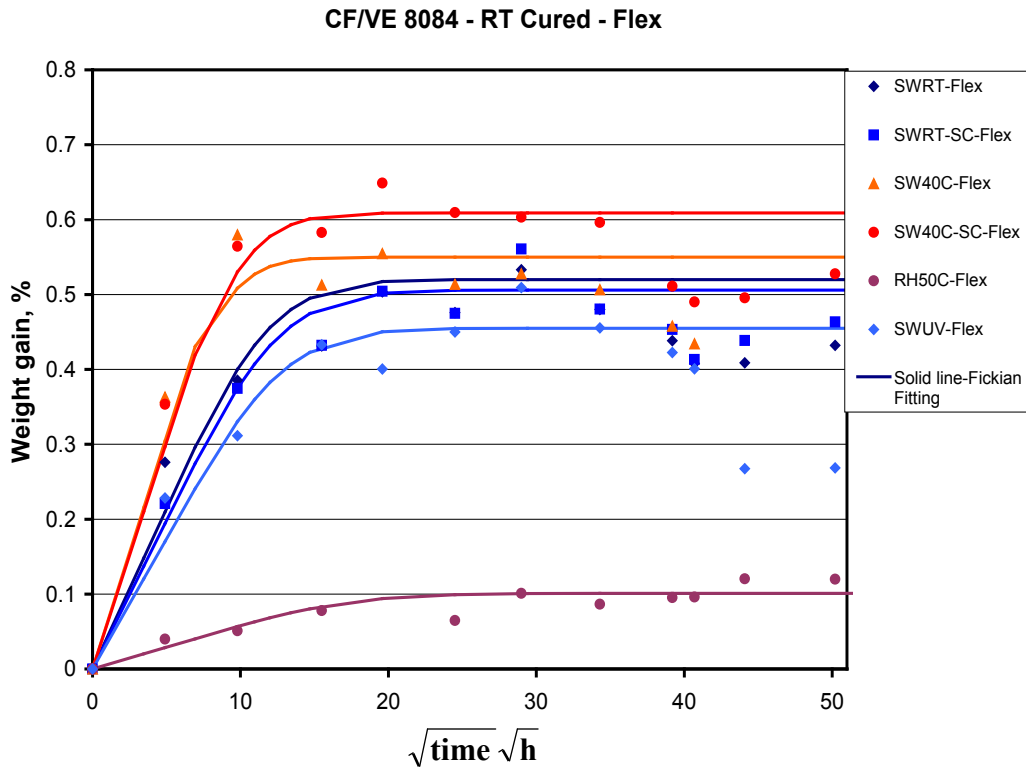
Figure 3.3: Moisture absorption curves for CF/VE8084 RT cured specimens

CF/VE 510A - RT Cured - Flex
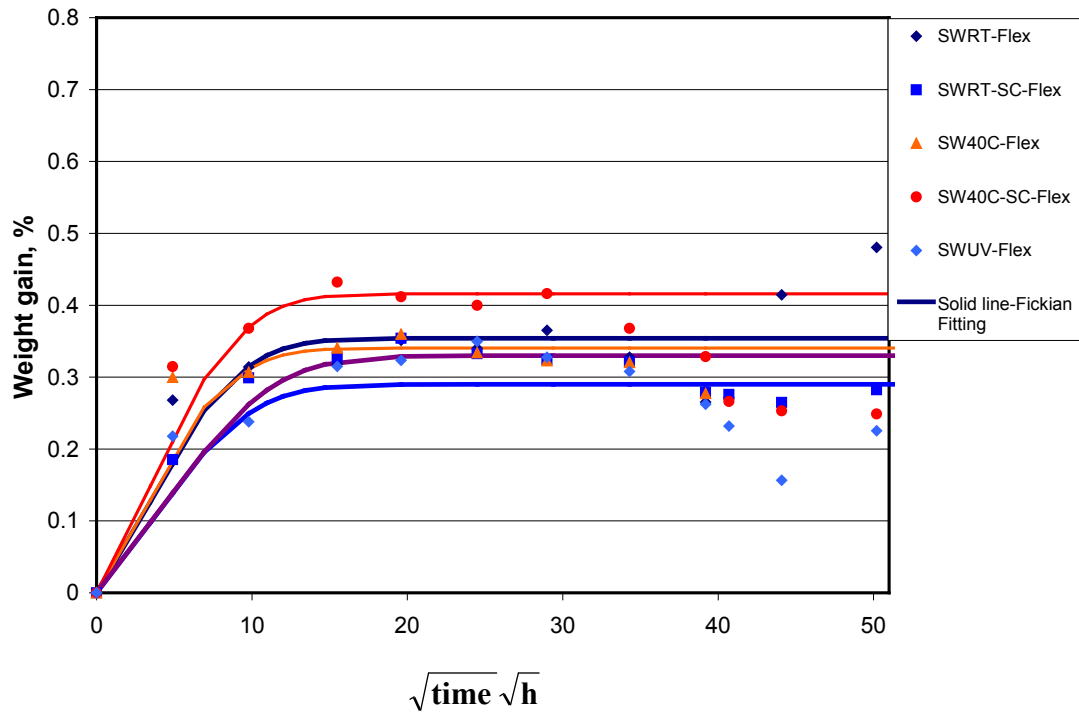
Figure 3.4: Moisture absorption curves for CF/VE510A RT cured specimens

Table 3.1 and 3.2 summarize the values of moisture saturation content (M%) and diffusivities (D) for each composite systems RT cured and post cured, respectively. Post cured samples slightly absorbs more water than the RT cured specimens, a plausible explanation for this could be attribute to a difference in the initial state prior to immersion. Post cured specimens were placed in the immersion tanks right after post-cure them, which means that the specimens were totally dried before immersion. To the contrary, the RT cured samples were immersed in the corresponding tanks after being sitting in the lab for two weeks, probably these specimens contain some moisture before

48

their immersion, which lead a difference in the starting point of the water uptake measurements between RT cured and post cured specimens. This fact justifies the lower moisture saturation content for the RT cured specimens.

Table 3.1: Maximum moisture contents and diffusivities values of composite specimens RT cured.

Environment	VE 8084-RT Cured		VE 510A-RT Cured	
	M %	D(m^2/h)	M %	D(m^2/h)
SWRT-SQR	0.29±0.01	2.5E-09	0.40±0.02	4.6E-09
SWRT-SC-SQR	0.26±0.01	3.5E-09	0.31±0.01	6.0E-09
SW40C-SQR	0.32±0.01	4.7E-09	0.45±0.03	5.9E-09
SW40C-SC-SQR	0.42±0.01	4.3E-09	0.45±0.02	6.8E-09
85RH50C-SQR	0.20±0.03	2.2E-09	--	--
SWUV-SQR	0.27±0.01	3.1E-09	0.35±0.05	3.4E-09
SWRT-Flex	0.53±0.03	4.3E-09	0.37±0.02	6.7E-09
SWRT-SC-Flex	0.56±0.02	3.4E-09	0.35±0.01	5.5E-09
SW40C-Flex	0.58±0.03	7.7E-09	0.36±0.03	7.2E-09
SW40C-SC-Flex	0.65±0.02	5.8E-09	0.43±0.03	6.6E-09
85RH50C-Flex	0.10±0.01	2.2E-09	--	--
SWUV-Flex	0.51±0.02	3.1E-09	0.35±0.03	4.4E-09

Table 3.2: Maximum moisture contents and diffusivities values of composite specimens post-cured.

Environment	CF/VE8084-Post cured		CF/VE510A-Post cured	
	M %	D(m^2/h)	M %	D(m^2/h)
SWRT-SQR	0.26±0.01	3.8E-09	0.40±0.01	4.5E-09
SW40C-SQR	0.37±0.01	4.1E-09	0.53±0.02	5.2E-09
85RH50C-SQR	0.30±0.01	3.4E-09	0.20±0.01	3.2E-09
SWRT-Flex	0.55±0.02	4.7E-09	0.51±0.01	5.9E-09
SW40C-Flex	0.69±0.001	5.9E-09	0.61±0.01	6.6E-09

The diffusivity characterizes the rate at which moisture is transported trough the material. As it will be discussed further, diffusivity depends on the fluid surrounding the material, on the temperature, on the specimen geometry or on the chemical composition of the material [64]. Other possible parameter that may influence the diffusivity is the state of stress of the material [64].

The solid lines in Figure 3.1-3.4 indicate the Fick's law fitting of the experimental data by using equation (1.4) and (1.3). In all the cases the fits are good.

The results listed in Table 3.1 and 3.2 show the D coefficient calculated. It is clear that, nevertheless the material, when the specimens are immersed in seawater the D increased when temperature increased, because diffusion is a thermally activated process [33]. Furthermore, water absorption is more rapid for the flexural specimens compare to the square specimens.

3.2   Mechanical testing

Three-point bending tests were performed on CF/VE510A and CF/VE8084 composite systems dried and after moisture saturation.

The flexural strength (X_2^F) results for both composite systems RT cured are listed in Table 3.3 and represented in Figure 3.5.

Table 3.3: Flexural strength of RT cured composites under different exposure conditions.

Environment	CF/VE 8084 RT cured			CF/VE 510A RT cured		
	M %	X_2^F (MPa)	% loss	M %	X_2^F (MPa)	% loss
Dry	--	712.1±15.3	--	--	791.5±45.9	--
SWRT	0.53±0.03	646.7±60.4	9	0.37±0.02	745.8±53.5	6
SW40C	0.58±0.03	622.2±61.3	13	0.36±0.03	740.7±17.2	6
85RH50C	0.10±0.01	642.3±86.0	10	--	766.9±36.0	3
SWUV	0.51±0.02	530.9±69.9	25	0.35±0.03	663.8±18.3	16
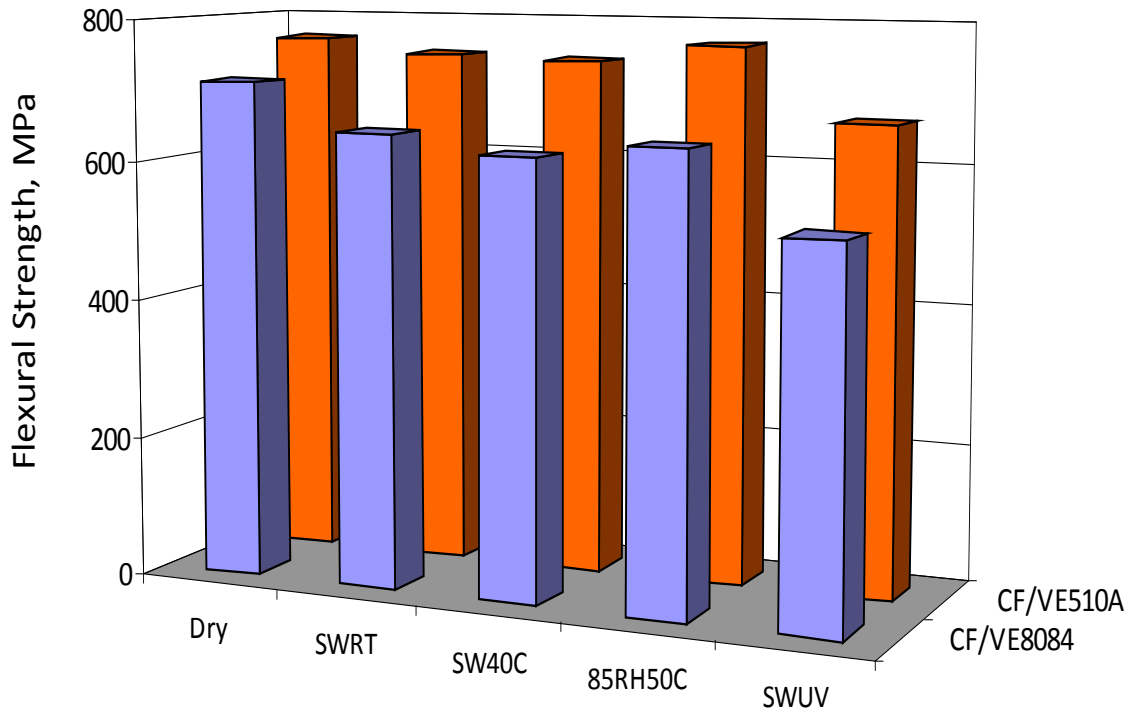
Figure 3.5: Flexural Strength of RT Cured composites under different exposure conditions

51

Reductions in flexural strengths after environmental exposure were evident for all composites. However, these reductions are more significant for the CF/VE8084 system compare to the CF/VE510A system. Any reduction due to moisture absorption of the flexural strength that is beyond the degradation of the matrix is attributed to F/M interface strength reduction [65]. Previous finding by Ramirez et al [52] on the same resin systems under studied reveals that the flexural strength data for these resins was not degraded by water absorption. Hence, the strength reduction observed for the vinylester matrix composites must be attributed to loss of F/M interface strength. However, the percentage loss in flexural strength (between 6-13%) are lower than the findings by other researchers, this could indicate that the F/M interface was degraded in a less extent. Kootsookos et al [8], for example, reported that flexural modulus and flexural strength were degraded by about 30%a and 40-50% respectively, for glass/vinylester composites immersed in seawater at 30^0C for two years.

Furthermore, composite specimens subjected to sprayed seawater and UV radiation experienced the largest reduction in flexural strength, 25% and 16% for CF/VE8084 and CF/VE510A systems respectively. Several researchers [12, 13, 14] have pointed out that when composites are exposed in seawater with the simultaneous UV radiation, a more severe degradation of the polymer composite might be possible. Bhavesh et al [15] reported that transverse tensile strength of carbon fiber epoxy composite was degraded by 29% when exposed in UV radiation (using QUV/Se weathering chamber) at 60^0C for 1000 hours. This exposure period is comparable to our case where composite were exposed to natural UV (sunlight), ambient temperature and seawater spray for approximately 1000 hours (assuming 12 hours of sunlight for 84

days). The flexural strength decreased by 25 % and 16% for CF/VE 8084 and CF/VE 510 systems respectively. These samples were subject to ambient temperature and for the exposure months the maximum temperature was ~35C. In addition to there degradation due to water up-take; these samples could also be subject to the photo-degradation.

Table 3.4 and Figure 3.6 summarize the results of flexural strength (X_2^F) for both composite systems RT cured after environmental exposure with the presence of stray currents and electrochemical interactions.

Table 3.4: Flexural Strength of RT cured composite under different electrochemical conditions.

Environment	CF/VE 8084 RT cured		CF/VE 510A RT cured	
	X_2^F (MPa)	% loss	X_2^F (MPa)	% loss
Dry	712.1 ± 15.3	--	791.5 ± 45.9	--
SWRT	646.7±60.4	9	745.8±53.5	6
SWRT/SC	604.1 ± 33.9	15	742.1 ± 25.9	6
SWRT/-0.6V	564.8 ± 55.8	21	707.2 ± 58.3	11
SWRT/Al	616.3 ± 22.3	13	663.7 ± 28.0	16
SW40C	622.2±61.3	13	740.7±17.2	6
SW40C/SC	624.6 ± 46.3	12	732.0 ± 41.0	8
SW40C/-0.6V	633.7 ± 29.7	11	863.8 ± 65.5	9*
SW40C/Al	651.5 ± 83.8	9	786.9 ± 49.1	1
85RH50C/Screw	664.9 ± 82.1	7	930.7 ± 77.6	18*

Note: * Positive value (i.e., Gain in strength)
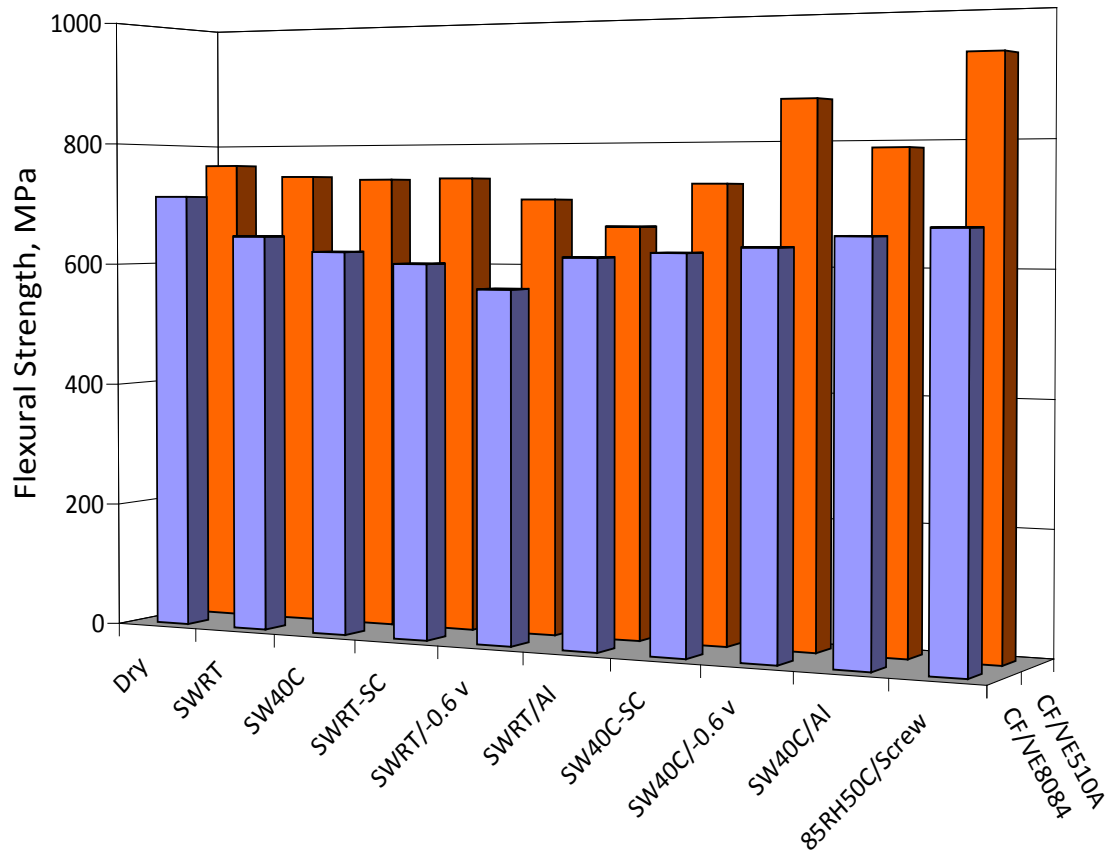
Figure 3.6: Flexural Strength of RT Cured composites under different electrochemical conditions

Composite specimens subjected to seawater combined with electrochemical interactions showed a decrease in flexural strength for all potential used and stray currents. At room temperature condition the reduction in the strength is more sever when electrochemical process are taking place and increases when the potential become more negative. However for exposure at 40^0C the loss in strength is comparable with the loss observed when no electrochemical interactions are present.

Once water and it dissolved oxygen reaches the surface of a carbon fiber the preferential cathodic reaction is the oxygen reduction reaction (at more negative potential

hydrogen evolution take precedence). The presence of electrochemical processes enhances the oxygen reduction reaction (ORR) that takes place at the carbon fiber / liquid interface which others have suggested that this causes degradation of the F/M interface due to hydrolysis. ORR produces OH^- ions which increase the solution pH, eventually this solution reaches the surface of the composite and allows the formation of calcareous deposits. Seawater has enough Ca and Mg compounds that could form calcareous deposits upon pH reaching an alkaline value, but this reaction does not take place in a neutral solution. The more negative the applied potential and particularly with an increase in temperature (faster thermodynamics of the reaction) allows for a faster formation of the calcareous deposits at the composite surface, functioning as an additional structural layer which acts reinforcing the composite material. However, it is possible that for specimens exposed in RT solutions did not have enough time to completely cover the specimens with calcareous deposits by the time the specimens were tested for flexural strength and thus showing worst performance when compared to no electrochemical processes present. In SW40C with stray current specimens had about the same flexural strength than those with no electrochemical process present. However, the flexural strength was larger for samples tested after exposure in SW40C and applied potential (-0.6 Vsce or -1.05 Vsce) than with no electrochemical process. For CF/VE 8084 (40C/-0.6 Vsce or -1.05 Vsce) the flexural strength was still lower than when compared to those tested dry, but for CF/VE 510A (40C/-1.05 Vsce) the flexural strength was about the same than dry, and a higher flexural strength was observed for CF/VE 510A (40C/-0.6 Vsce). An increase in flexural strength rather than decrease was also observed for CF/VE510A composite system exposed at 85RH50${}^{\circ}$C with galvanic couple.

Three-point bending test was also performed on post-cured composite specimens. Tables 3.5-3.6; and Figures 3.7-3.8, depict the flexural results obtained for CF/VE8084 and CF/VE510A, respectively.

Table 3.5: Flexural strength of RT cured and post-cured CF/VE8084 composites under different exposure conditions.

Environment	CF/VE8084, X_2^F (MPa)			
	RT Cured	%loss	Post Cured	%loss
DRY	712.1±15.3	--	891.3±76.4	--
SWRT	646.7±60.4	9	722.0±10.2	19
SW40C	622.2±61.3	13	679.3±18.6	24
85RH50C	642.3±86.0	10	836.7±17.7	6

Table 3.6: Flexural strength of RT cured and post-cured CF/VE510A composites under different exposure conditions.

Environment	CF/VE510A, X_2^F (MPa)			
	RT Cured	%loss	Post Cured	%loss
DRY	791.5±45.9	--	938.4±32.9	--
SWRT	745.8±53.5	6	847.3±44.1	10
SW40C	740.7±17.2	6	834.2±19.6	11
85RH50C	766.9±36.0	3	894.6±69.5	5
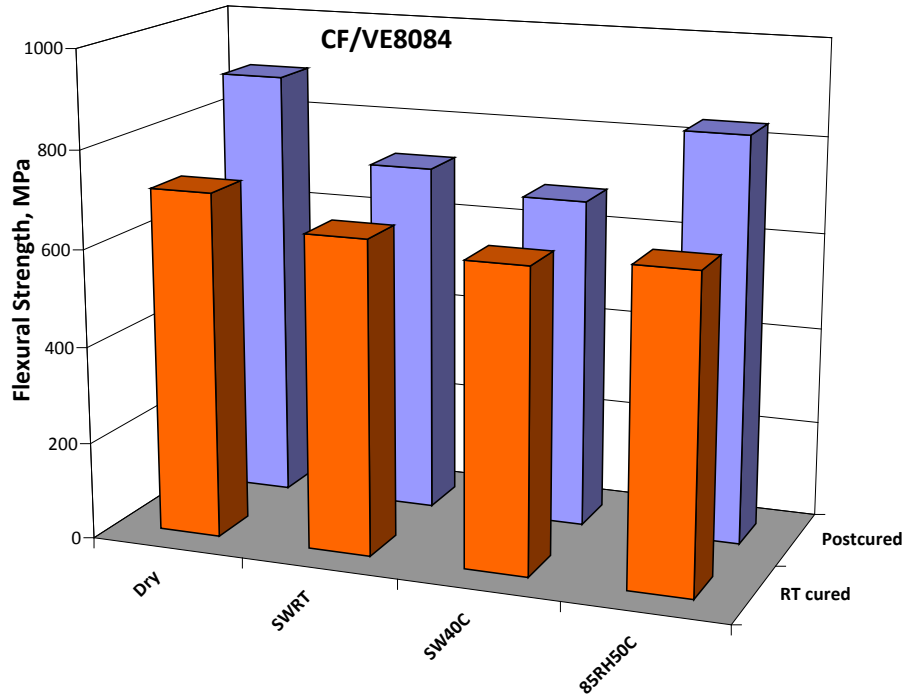
Figure 3.7: Room Temperature Cured and Post Cured effects on Flexural Strength of Composites (CF/VE8084)
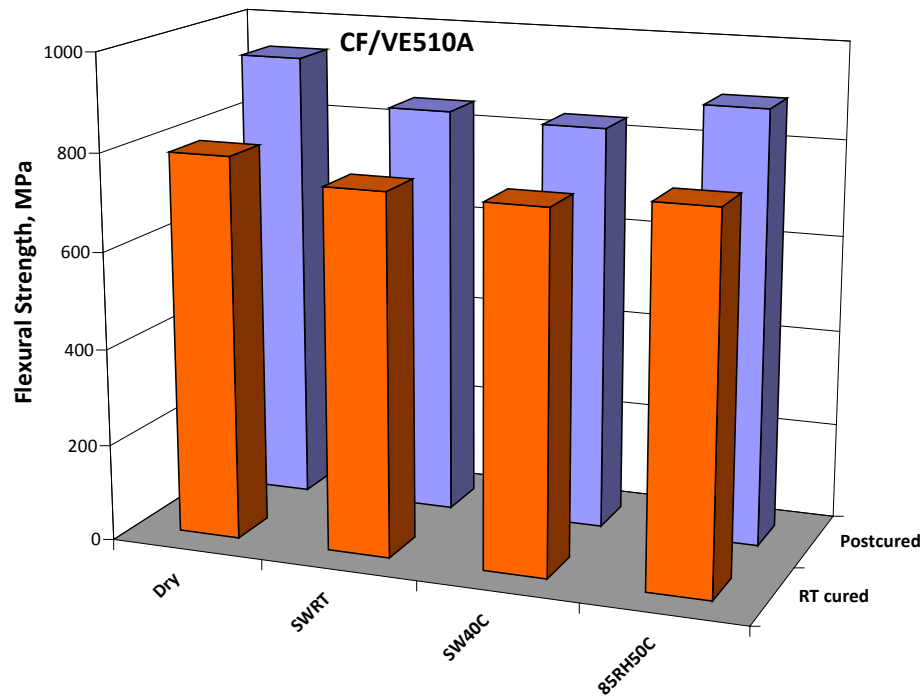
Figure 3.8: Room Temperature Cured and Post Cured effects on Flexural Strength of Composites (CF/VE510A)

As can be observed the mechanical properties are significantly affected when post-cure is performed on the composite materials. Flexural strength increased by 20% and 16% for CF/VE8084 and CF/VE510A systems at dry conditions, respectively. However, when post-cured specimens are subjected to marine environments the flexural strength is degraded in more extent than when specimens were RT cured.

3.3   Optical micrographs

Selected areas of the flexural specimens were examined by optical microscope. Figure 3.9 (a) shows typical cross-section of the composite before fracture, top picture shows the cross-section for a cut perpendicular to the fibers direction and the bottom picture the cross-section for a cut parallel to the fibers direction [57] and figure 3.9 (b) shows a picture from the literature [58] of a cross-ply composite, in this picture compression microbuckling is observed (light gray in here is matrix).
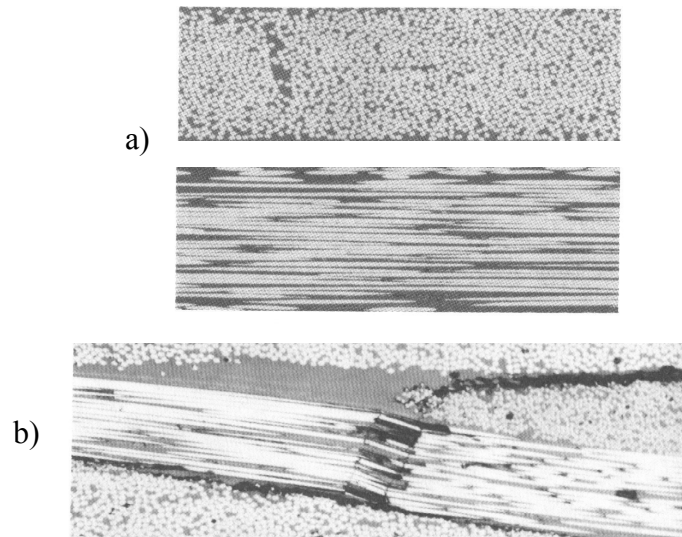
Figure 3.9: a) Cross-sectional optical micrograph of composite materials before failure [57] b) After failure [58]

Figures 3.10 and 3.11 show the optical micrographs of CF/VE 510A composite at dry and after SW and UV exposure conditions, respectively. Specimens were cut half way along the longitudinal (fiber) direction (i.e. cross-section parallel to fiber direction).
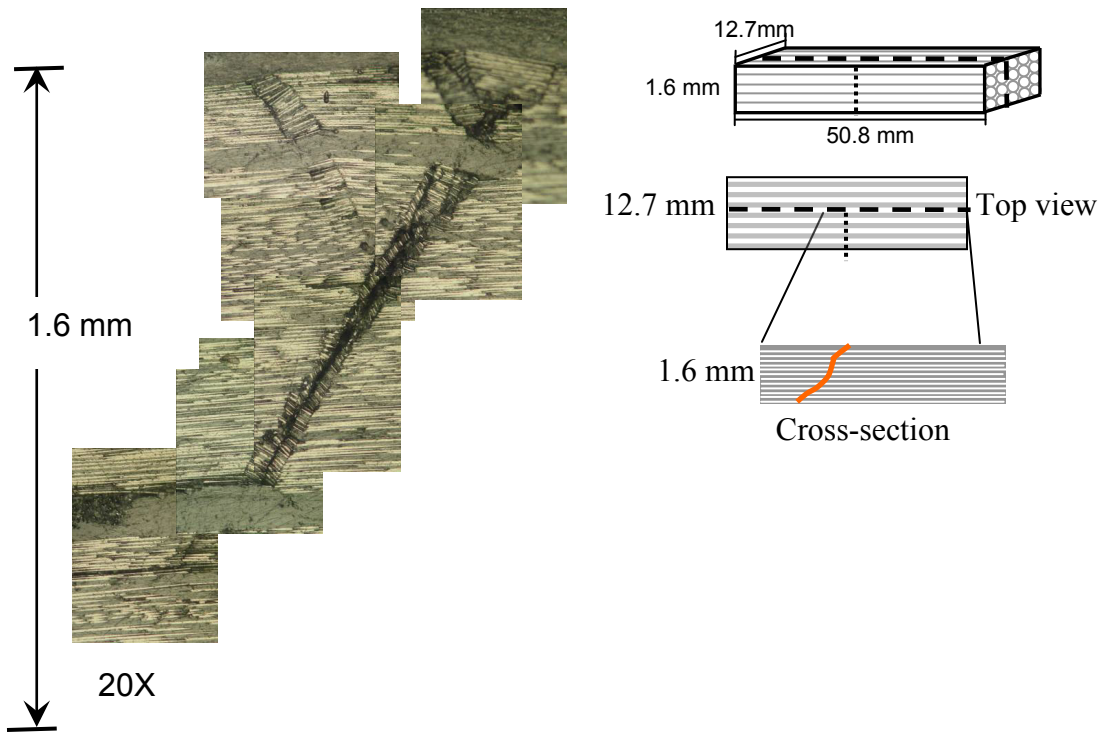
Figure 3.10: Cross-sectional area of the flexural tested CF/VE 510A specimen in dry conditions. (This picture is a collage of several pictures each taken at 20X)

It can be observed fiber breakage and matrix cracking through the thickness direction, indicating that the failure mechanism was not that of a fiber pullout or interface failure (at least at this magnification). This, however, is expected, as fiber pullout requires a tensile stress. These fracture surfaces were created as a crack grew through the thickness of the material. Based on the visual observation; it is speculated that the crack

59

initiated on the top surface at the point of load application (compression site). This crack then grew downward, fracturing both the matrix and fiber material. The crack may have been initiated by microbuckling of fibers attributable to the local stress concentration induced by the loading point. This fiber microbuckling was noted as a failure mechanism in other studies using a bend test to study composites with thermosetting matrices [56].
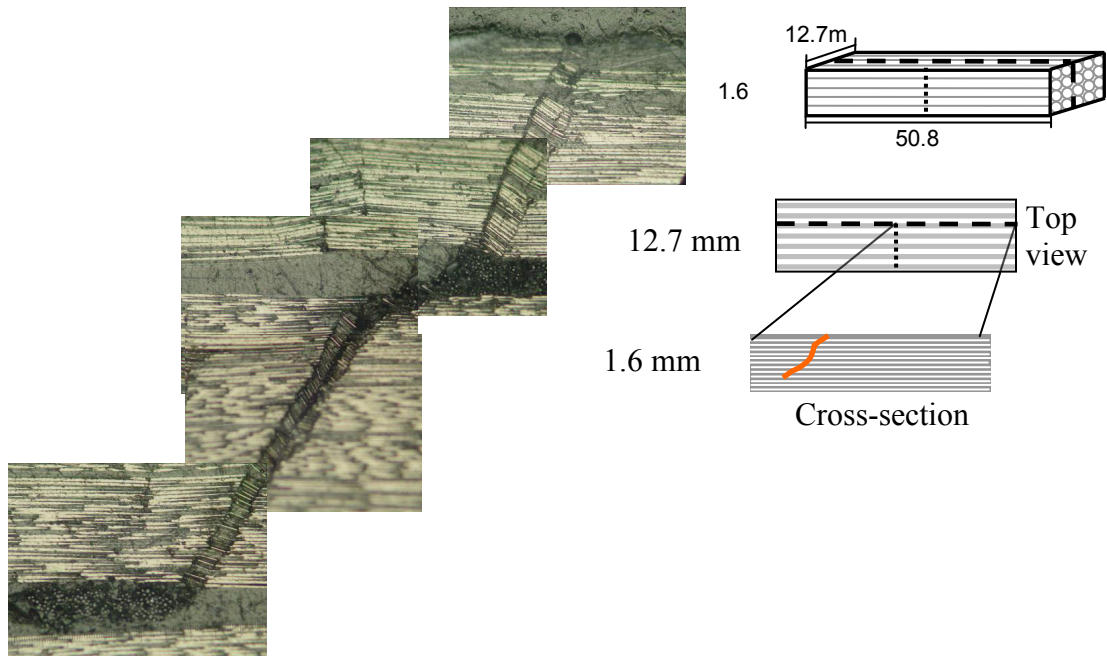
Figure 3.11: Cross-sectional area of the flexural tested CF/VE 510A specimen exposed to SW and UV radiation. (This picture is a collage of several pictures each taken at 20X)
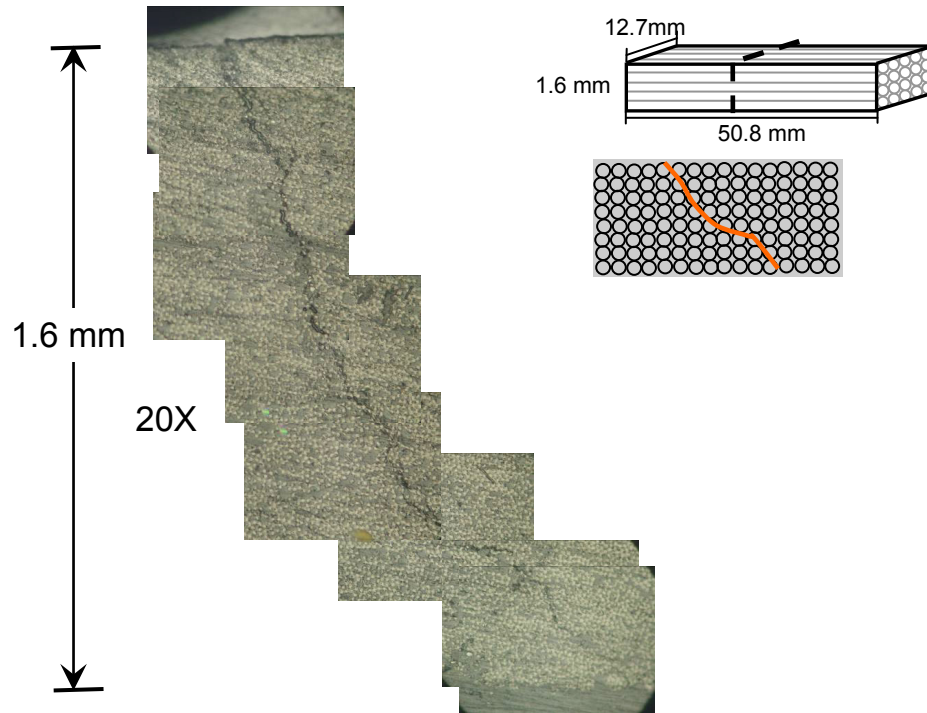
Figure 3.12: Failure surface the flexural tested CF/VE 8084 specimen exposed to SW and UV radiation. (This picture is a collage of several pictures each taken at 20X)

Same failure trend was observed for dry and SW and UV exposure conditions. Figure 3.12 shows the optical micrograph of CF/VE 8084 composite after SW and UV exposure. In this case, specimen was cut half way perpendicular to the fiber direction, close to the compression site. From the cross-section of the tested specimen it can be also observed that matrix cracking occurs along the specimen thickness.

3.4 EIS results

3.4.1 EIS spectra

Measurements conducted on day 0 for all cases started by filling the EIS cell reservoir with seawater at room temperature. Typically 20-60 minutes passed before running the EIS test. The samples that were exposed for slightly longer time might have allowed for some water uptake and hence resulted in a lower impedance magnitude observed at the low frequency end of the spectra in some of the cases described below. The transition to lower impedance magnitude was actually observed during some of the day 0 EIS runs. Most of the samples used were only sealed on the side where the electrical connection was made, only for selected cases were all edges sealed with a marine sealant.

Figure 3.13: Bode magnitude and phase angle for CF/VE composite in seawater at RT

Figure 3.13 shows the Bode magnitude and phase data at different exposure time for CF/VE composite exposed in seawater at room temperature. Initial impedance magnitude values at low frequency were close to $10^7 \Omega$-cm^2 for both resin systems. After one day of immersion, the impedance magnitude shifted to $10^6 \Omega$-cm^2 for the 510A resin system while the magnitude shifted to below $10^5 \Omega$-cm^2 for the 8084 resin system. The impedance magnitude measured at lower frequencies decreased with time, reaching values below $10^4 \Omega$-cm^2. At the high frequency end of the spectra the impedance magnitude increased with time.

With respect to the phase angle one peak was observed at day 0 and day 1. Two or more time constants appeared to be present from the phase diagrams obtained after 4 days of immersion. At low frequencies the phase angle was smaller than 20 degrees for the 8084 resin system, a similar trend was observed for 510A resin system except for day 33 in which a phase angle peak greater than 30 was observed at low frequencies. At high frequencies the phase angle shifted to lower values for both resin systems except on day 63 for 8084 resin system. In addition, as the time progressed, Bode phase data showed two time constants for 510A resin system, one being at the high frequency region and other at the lower frequency.
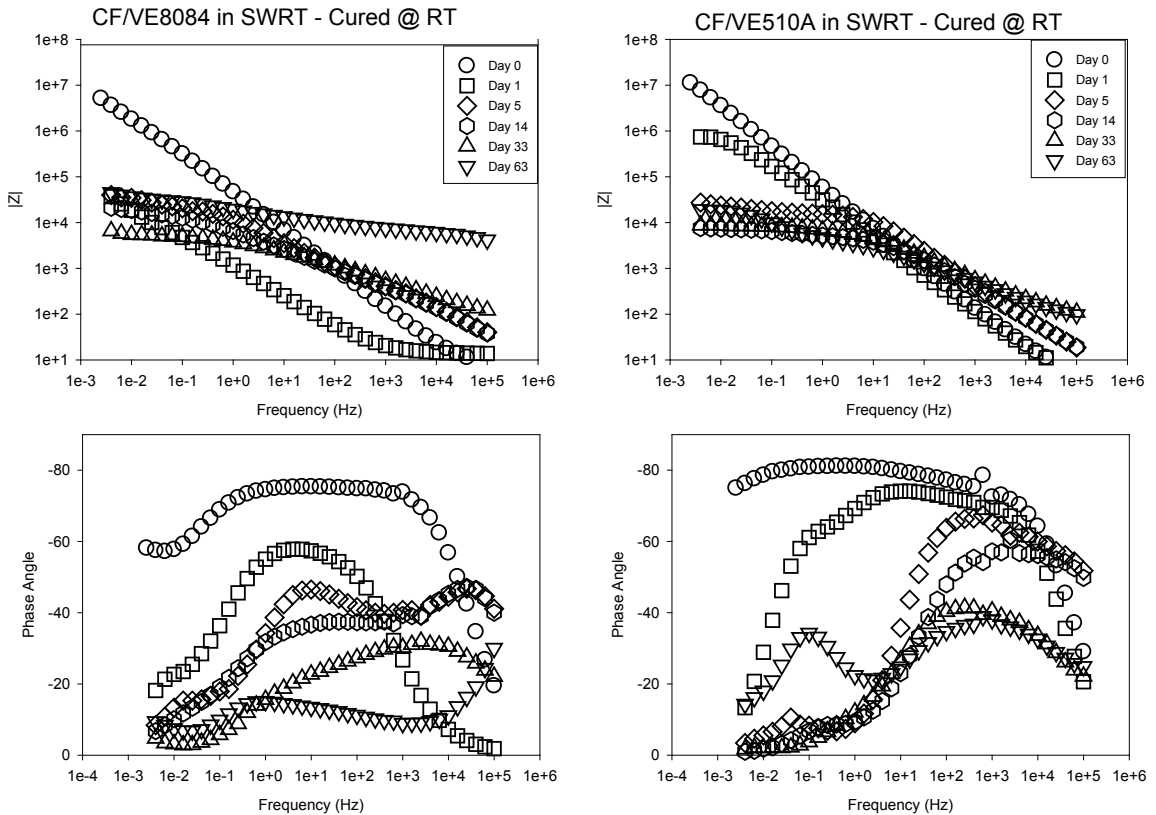
Figure 3.14: Bode magnitude and phase angle for CF/VE composite in seawater 40C

Figure 3.14 shows the Bode magnitude and phase data at different exposure time for CF/VE composite immersed in seawater at 40^0C temperature. Initial impedances magnitude at low frequency was below $10^7\Omega$-cm^2 for 8084 resin system while above $10^7\Omega$-cm^2 for 510 resin system. At high frequency impedance magnitude decreased with time. After one day, low frequency phase angle was smaller than 20 degrees for both resin systems except the day 33 for 8084 resin system in which phase angle peak greater than 20 degrees was observed in at low frequency. At intermediate frequencies (10-1000 Hz) of the spectra, phase angle data shifted to lower phase angle values for both resin system. Moreover, as the time progressed, Bode phase data showed two time constants

for 510A resin system, one being at high frequency region and other at the lower frequency. The same trend was observed for 8084 resin system but in case of day 14, 33 and 63. Furthermore, initial phase data showed simple RC constants for both resin system.

Figure 3.15: Bode magnitude and phase angle for CF/VE post cure composite in seawater 40C

Figure 3.15 shows the Bode magnitude and phase data at different exposure time for CF/VE composite exposed in seawater at 40^0C temperature for post cure specimens. After one day of immersion, the impedance magnitude shifted to below $10^5\Omega$-cm^2 and this trend is quite similar for both resin systems. At high frequency end of spectra the impedance magnitude slightly increased with time. The phase angle spectra for 510A

65

system remain very similar after 1 day, peak on the high frequency end move to lower values but maintain its position at about 1E+3 Hz whereas the peak on the low frequency end increased with time and shifted slightly towards lower frequencies. For samples made with 8084 the phase angle curves was very different at day one, with the spectra obtained on day 4 being very similar in shape to those observed for the 510A system. At later dates the peak at the high frequency end shifted to lower frequency values, and possibly also this took place for the peak at lower frequencies but this shift is not very evident from the plot.
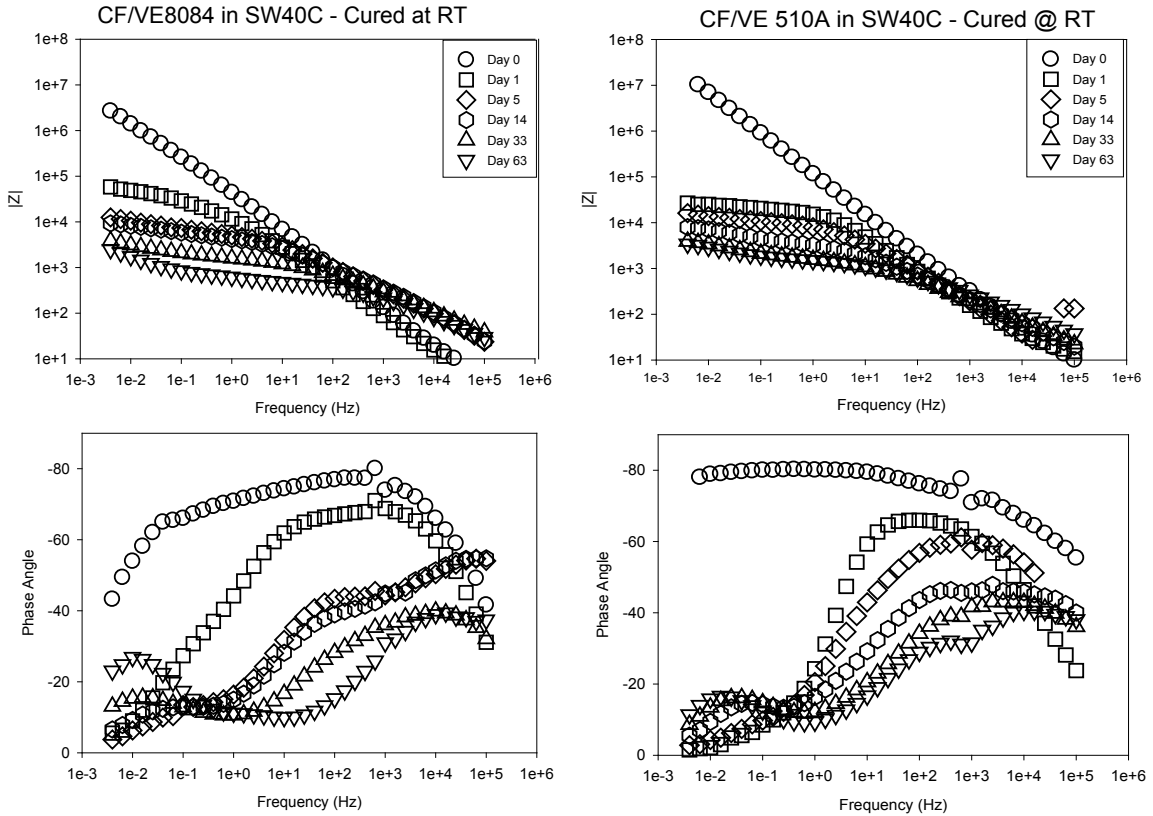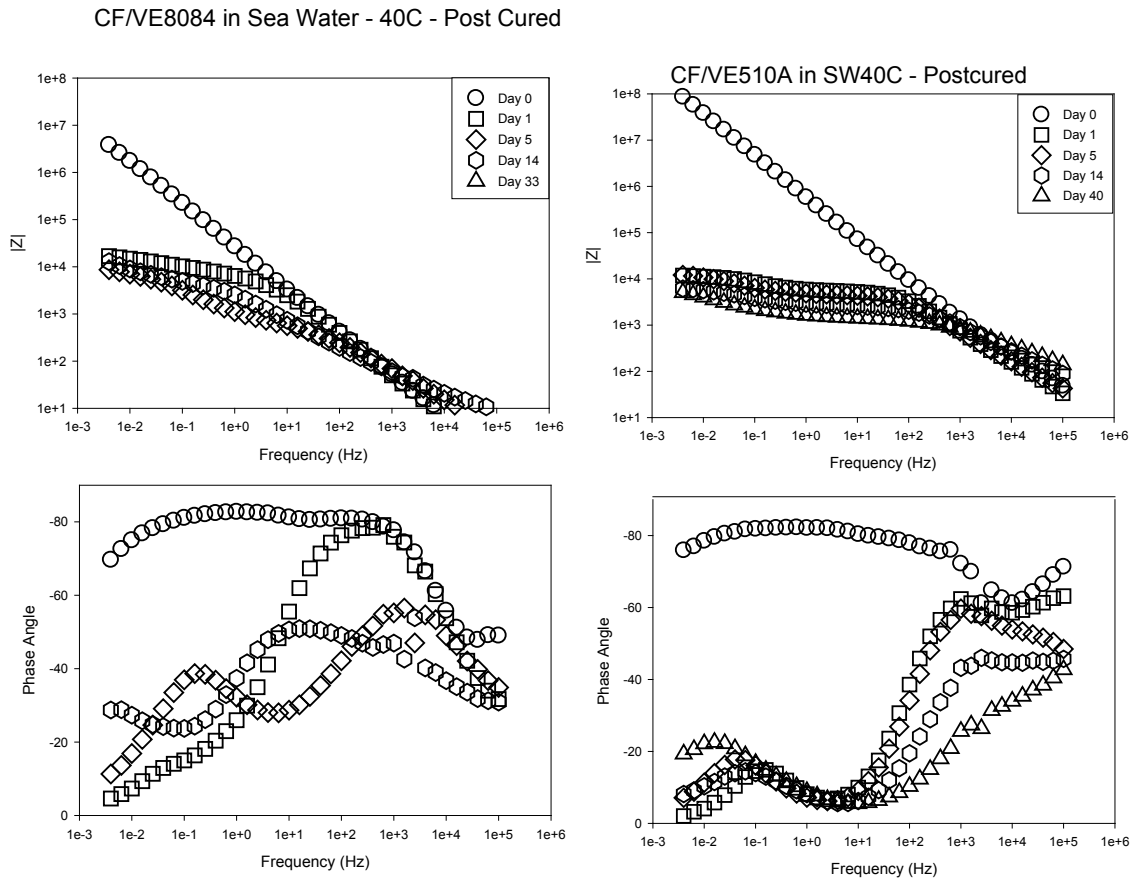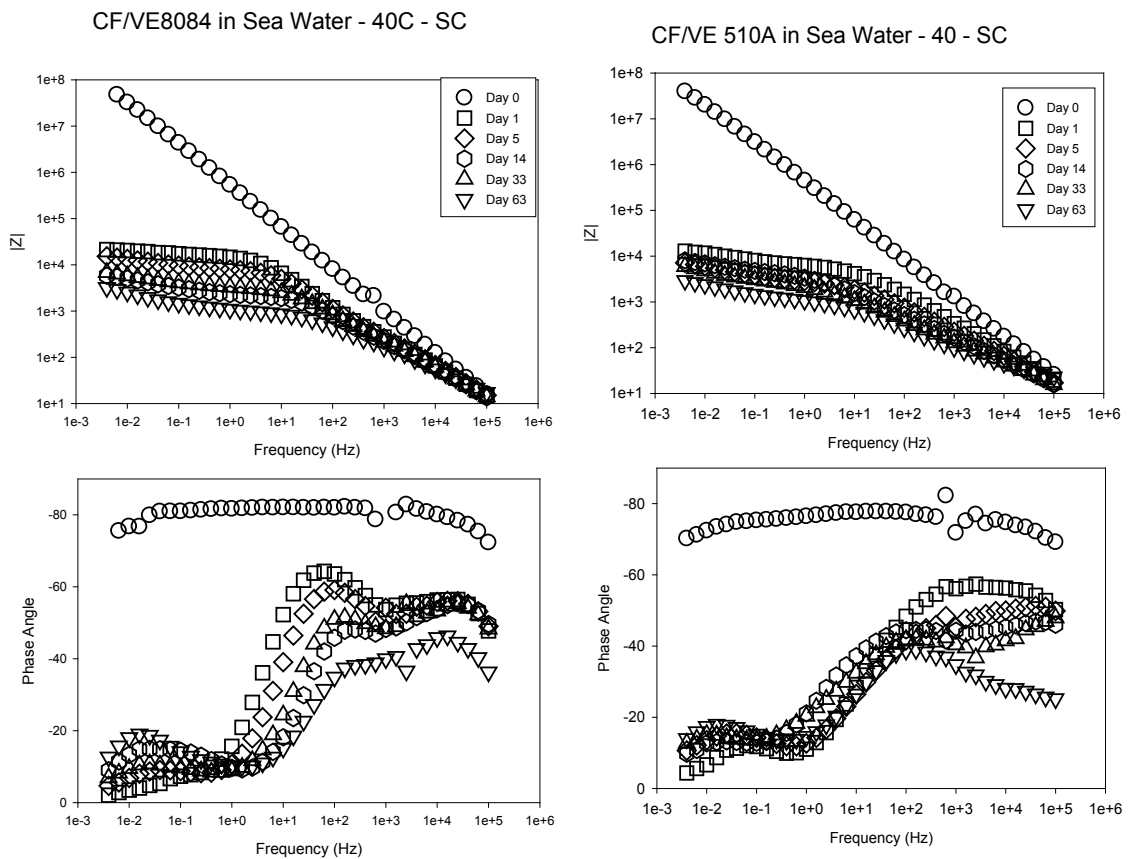

Figure 3.16: Bode magnitude and phase angle for CF/VE composite in seawater at 40C-stray current

Figure 3.16 shows the Bode magnitude and phase data at different exposure time for CF/VE composite exposed in seawater at 40^0C temperature at stray current condition. After day one, impedance magnitude shifted from $10^8\Omega$-cm^2 to below $10^5\Omega$-cm^2 for both resin systems. The impedance magnitude monotonically decreased with time at low frequency. The shape of the phase angle spectra after one day is very different from those described above. Having the stray current present appears to add a third time constant. Bode phase data clearly shows three time constants, one at low frequency, one at intermediate frequency and another at high frequency and its observed from day 1 to day 63. These time constants are easier to observe on the 8084 system by the three peaks present and likely are also present on the 510 system. At low frequency phase angle was smaller than 20 degrees for both resin systems, but the peak tended to increase as exposure time increased. At intermediate and high frequencies the phase angle moved towards lower values for the 8084 system, but the peak remained at about the same frequency locations. For the phase angle for 510A resin system, phase angle shifted to slightly higher values at intermediate frequencies and at high frequencies it moved towards lower phase angle values. In addition, for 8084 resin system, day one phase data showed simple RC constants for both resin system.

The appearance of third time constant is may be due to the effect of stray current. Further tests are being conducted to understand the effect of stray current on the composite degradation.

Figure 3.17: Bode magnitude and phase angle for CF/VE composite in seawater at 40C- galvanic coupling-0.6V

Figure 3.17 shows the Bode magnitude and phase data at different exposure time for CF/VE composite exposed in seawater at 40^0C –Galvanic coupling (Applied potential -0.6V) condition. Initial impedances magnitude values at low frequency were below $10^6\Omega$-cm^2 for both resin system, this is likely due to a longer initial exposure time to seawater solution before running day o EIS scans. At high frequency end of spectra impedance magnitude decreased with time for both resin system. The magnitude diagram

for 510A system on day 63 showed a significant increase in impedance at all frequencies, it is possible that enough calcareous deposits formed between day 14 and day 63 to produce this impedance shift. The phase angle diagrams show that polarization

to -0.6 Vsce produce somewhat similar diagrams to those observed for samples exposed to stray current. There are a few differences for instance the peak at the high frequency end of the spectra is not easy to see, except for a change in the slope. At intermediate and high frequencies (i.e. > 10 Hz), the phase angle shifted to lower values for both resin system. At day 63, the phase angle diagram at high frequency region is very distinct and are the lowest values observed for both systems while at low frequencies there is an increase in the phase angle for 8084 sample whereas the angel is almost nil for the 510A system.
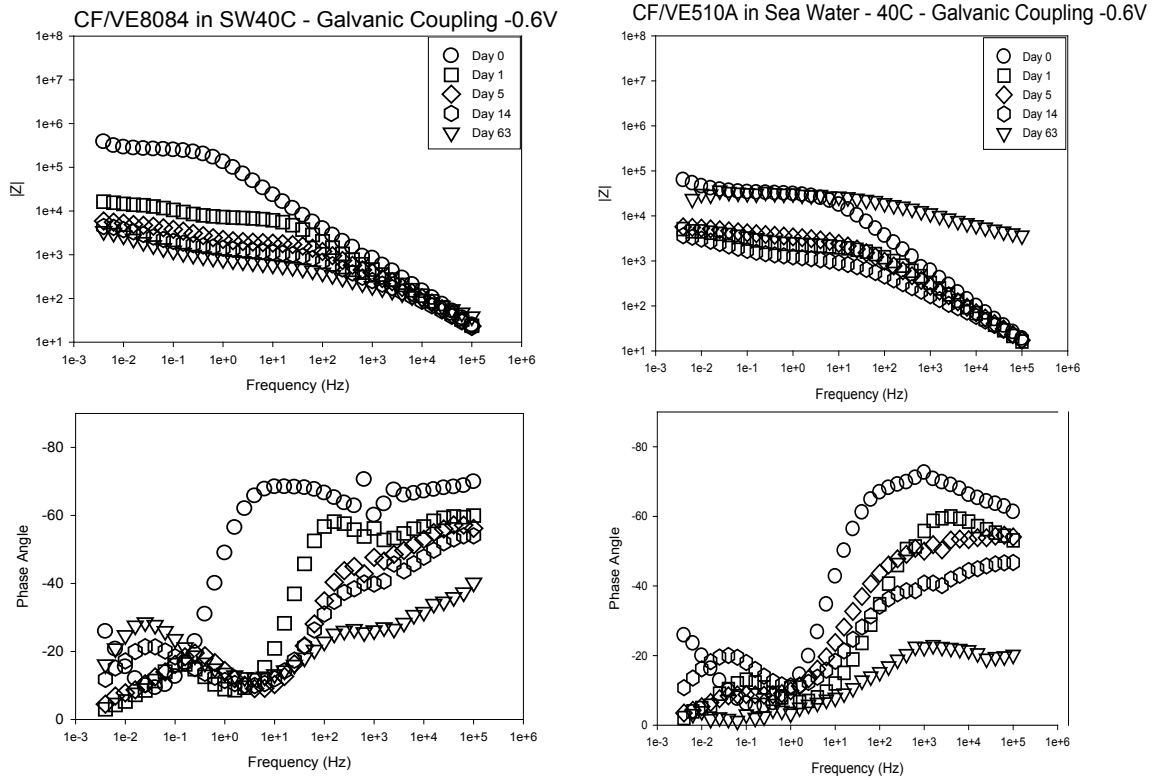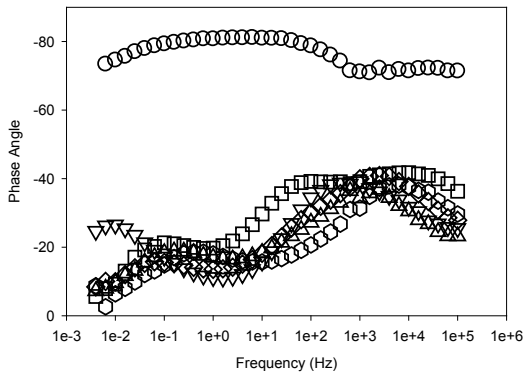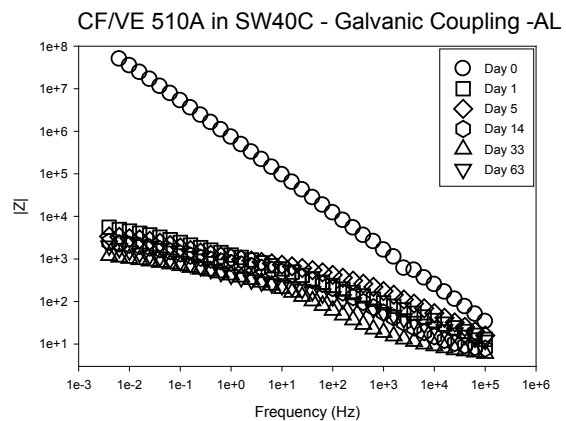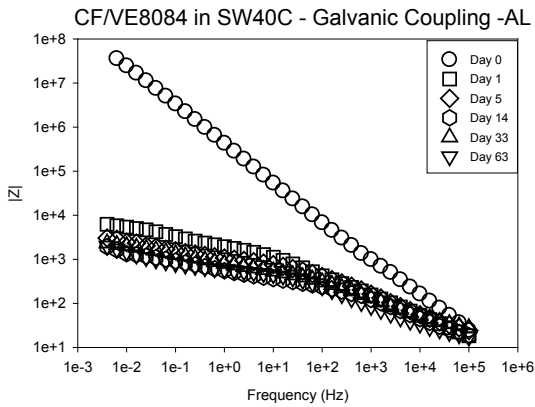
Figure 3.18: Bode magnitude and phase angle for CF/VE composite in seawater at 40C-
Galvanic Coupling-Aluminum

Figure 3.18 shows the Bode magnitude and phase data at different exposure time for CF/VE composite exposed in seawater at 40^0C –Galvanic coupling (Aluminum anode) condition. After one day of immersion, the impedance magnitude shifted from $10^8\Omega$-cm^2 to $10^4\Omega$-cm^2 for both resin systems. At high frequency the impedance magnitude decreased with time for both resin system, except for day 63 510A system, there was slight increase in the magnitude at higher frequencies. After one day of exposure the maximum phase values observed was about 40, significantly lower than any of the previous cases shown. At low frequencies phase angle was smaller than 20 degrees except the day 63 for both resin system in which a phase angle peak greater than 20 degrees was observed. At high frequencies phase angle peak moved to the lower frequencies for both resin system. In addition, Bode phase data showed two time constants for both resin system; one is being at low frequency and other being at high frequency.
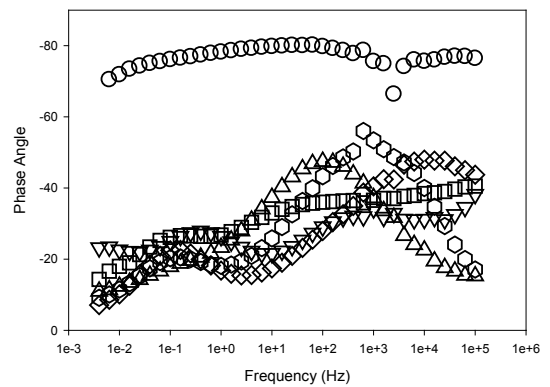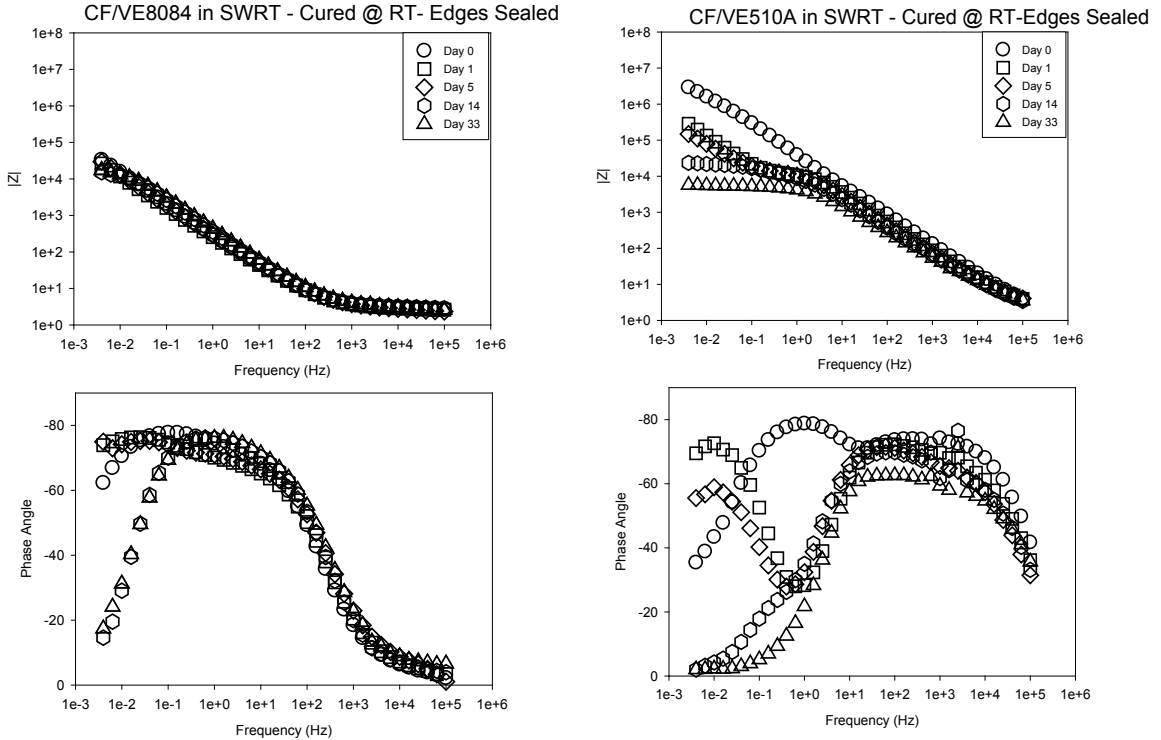
Figure 3.19: Bode magnitude and phase angle for CF/VE composite in seawater at room temperature with edges sealed

Figure 3.19 shows the Bode magnitude and phase data at different exposure time for CF/VE composite exposed in seawater at room temperature with edges sealed. Initial impedances magnitude at low frequency was below $10^5 \Omega$-cm^2 for 8084 resin system while above $10^6 \Omega$-cm^2 for 510 resin system. Both samples likely were exposed for an extended period of time before initiating the EIS testing. Almost no further reduction in impedance magnitude at the lower end of the frequency spectra was observed on the 8084 system, whereas a monotonic reduction in impedance magnitude was observed for the 510A system. The Bode diagram shows very distinctive spectra for the 8084 system, showing a typical RCR type of model. The tested sample from the 510A system showed two time constants at day 1 and day 4, but reduces to a RCR circuit for day 14 and 33.

71

These diagrams are very similar to what has been reported by the URI group, where the water only penetrates from one face since a small volume is present at all times, whereas all samples tested in here were fully immersed in relatively large seawater tanks.

For all environmental and electrochemical conditions, the change in the high frequency spectrum was more dramatic and sensitive to the ingress of moisture into the composite.

3.4.2 Equivalent circuit modeling

The following paragraphs describe possible physical model interpretations as equivalent circuits for the systems investigated in this thesis. As the frequency changes from high to low it allows to observe the various physical components present in the system. The solution resistance is usually identified as the impedance magnitude observed at the high frequency end of the spectra.

For the cases in which there is no polarization: a possible electrical circuit that describe the physics of the model is shown below in figure 3.20. Rs is the solution resistance (in this case seawater). The matrix could be seen as a coating that has two components 1) resistance Rpo (i.e. the resistance of the polymer matrix that can tend to lower values (observed in all) due to penetration of electrolyte through pores or due to weaking and 2) a capacitance (or constant phase angle) due to the polymer dielectric constant (which likely increase as water uptake occurs). The inner circuit describes the contributions at the carbon fiber/moisture interface region (also known as double layer capacitance shown as with label Q_{dl} in the diagram) and Rt is the charge transfer at the carbon fiber/polymer interface. (The inner circuit might not be present in cases where the

72

moisture has not reached the interface). Numerical fitting was conducted to try to identify values that could better describe the experimental observations. Low Rp values in the case of metals with coatings are indicative of bad coatings. In the case of the CF/VE composites the multiple fibers present could be seen as potential sites that have a distributed cover thickness, water could reach some fiber before others, which is analogous to something called a transmission line due to multiple capacitor and Rt values, in some cases all these components can be represented by the inner circuit, but not always.
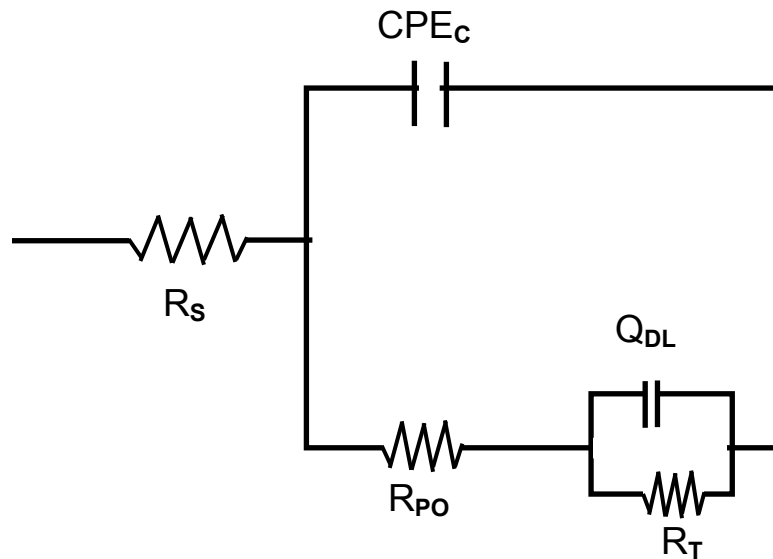

Figure 3.20: Proposed equivalent circuit for cases in which there is no galvanic coupling or stray currents.

Based on research performed by D Aylor and J Murray in early 1990's immersing a CF/VE composite sample in seawater could be considered a coating with pores (polymer matrix covering the outer carbon fibers) which can allow with time the

transport of seawater to reach the reinforcing carbon fibers. Once this electrolytic path has formed; the carbon fibers surface (specially when coupled to a metal Al anode or polarized via a power supply -0.6 Vsce) become oxygen reduction reaction areas for the galvanic couple. The resulting alkalinity from the oxygen reduction reaction can allow precipitation of magnesium and calcium compounds which as time passes could form visible calcareous deposits coating. This coating could act as an additional electrical capacitor. The calcareous deposits if very compact are likely to have low porosity which would limit the seawater reaching the carbon fibers which in effect would act as an additional electrical resistor (Rcal-pore), additionally the presence of this coating could reduce the amount of solution transported into the matrix resulting in a higher Rpo.

At the potentials values at which the CF/VE composites were polarized there is the possibility of mass transport limitations (a balance between the amount of O_2 reaching the CF and the amount of oxygen that is consumed) or diffusion control. Figure 3.21 shows equivalent circuits proposed by Aylor et. al. [59] when the composite is galvanically coupled. Case a) has three time constants (or capacitors type components) as observed in some of our results. For some situations the model can be simplified as seen on second diagram (b) with a model with only two time constants in which the parallel capacitors are combined in one.

a)

C poly

C calc

Rs

QDL

R calc pore   R poly pore

RT

Where

C_{poly} = capacitance (polymer)

C_{calc} = capacitance (calcareous deposit)

R_S = solution resistance

$R_{calc\ pore}$ = resistance (pores in calcareous deposit)

$R_{poly\ pore}$ = resistance (pores in polymer)

Q_{DL} = double layer capacitance

R_T = charge transfer resistance

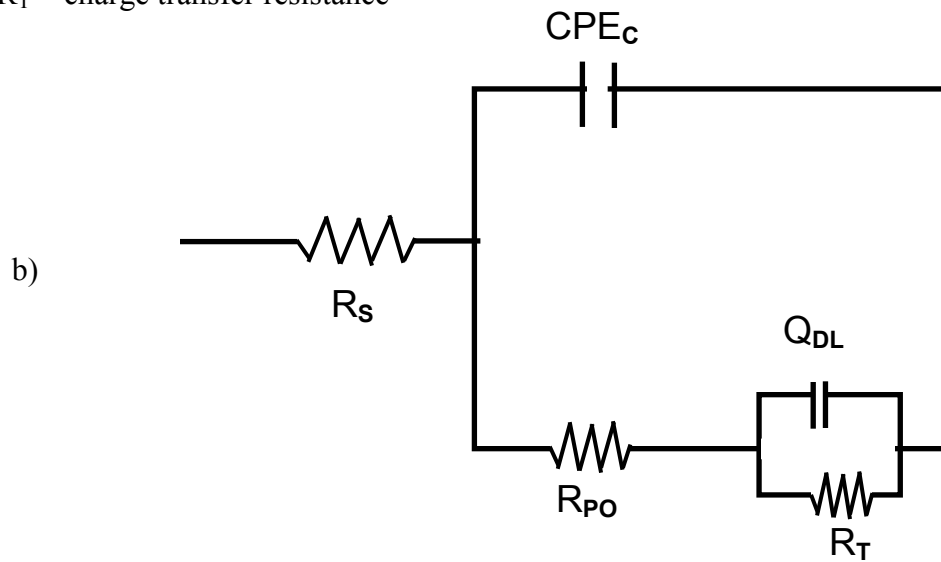CPE$_C$

Rs

b)

QDL

RPO

RT
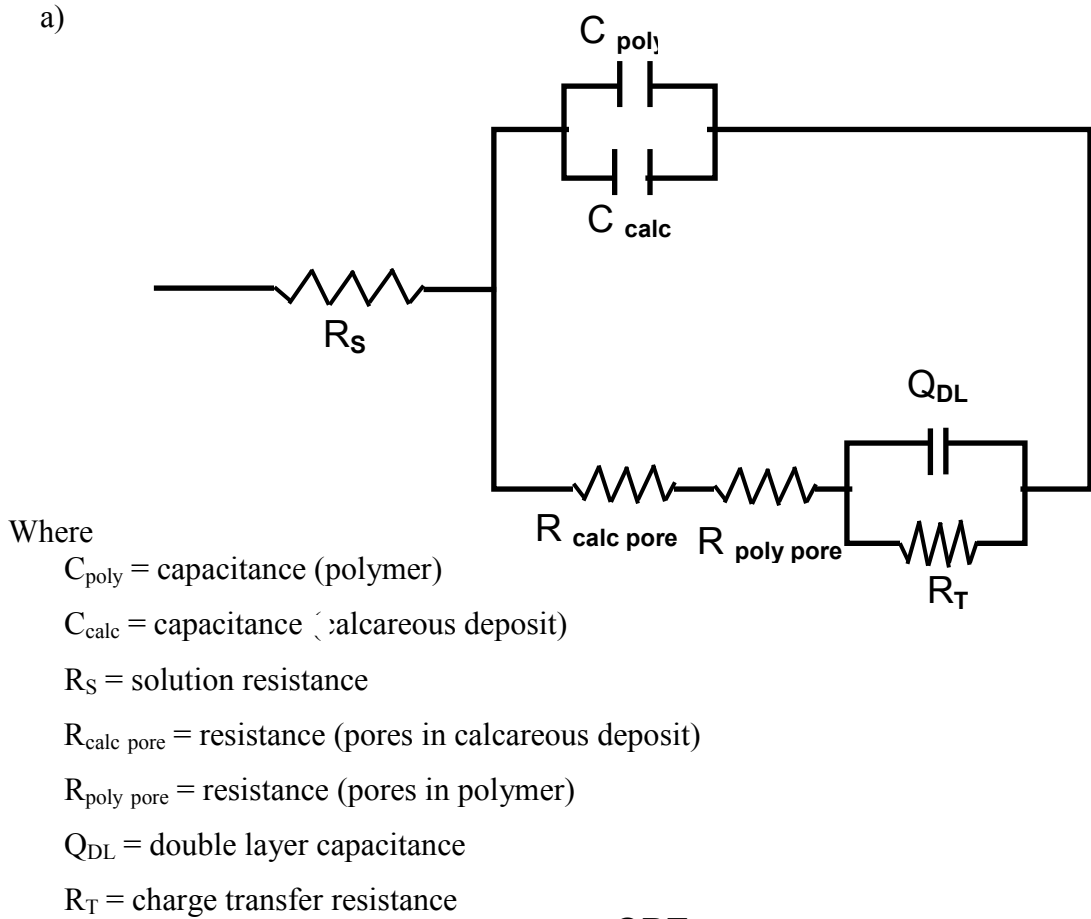
Figure 3.21: Equivalent circuits for cases with galvanic coupling.

3.4.2.1 Modeling fitting

EIS data obtained from individual scans were analyzed using Boukamp software. This computer program uses complex nonlinear least squares (CNLS) regression technique. Equivalent circuits were chosen in such a way that it qualitatively described the physical behavior of the system under test. Initial estimates of the circuit element were obtained based on values observed on each spectra. The CNLS program iterate multiple times until the error is small or does not change anymore .Finally the best fit computed patameters were used to generate an impedance spectrum for comparison with the experimental EIS data. Selected cases for 8084 resin based composites were chosen for equivalent circuit modeling.

Equivalent circuits as shown in figure 3.22 were used to model the EIS data obtained for the composites when treated as electrode. The choice of the simplified equivalent circuit gave the ease in estimating the initial guesses and also facilitated in performing the fitting quiet easily.

a)

b)
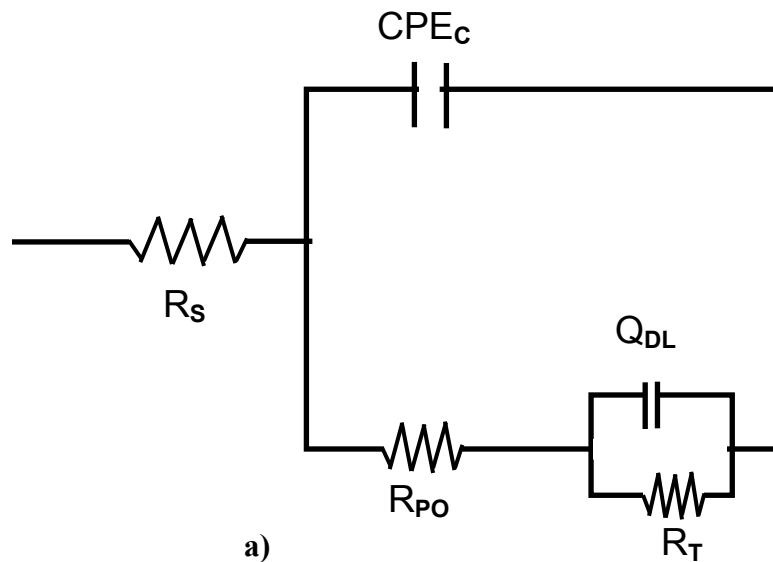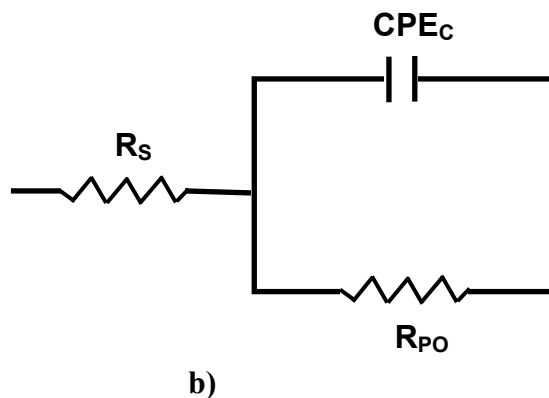
Figure 3.22: Equivalent circuit used for fitting EIS data

A constant phase element (CPE) was chosen to model the capacitive behavior of the polymer matrix. A constant phase element models the behavior of a double layer, that is an imperfect capacitor. A typical CPE response characteristic is to have a depressed semi-circle on the complex impedance plane. The impedance response of the CPE is governed by the following equation:

$$Z_{CPE} = \frac{1}{T(j\omega)^n}$$

Where n is a real number between 0 and 1. CPE acts like a capacitor with T=C when n=1. R_S is defined as the solution resistance while CPE_C is the constant phase element representation for the capacitance of the polymer matrix. R_{PO} is the electrical resistance through the polymer. The term pore resistance, R_{PO} was attributed to the measured resistance of the inhomogeneous polymer matrix any electrolyte transported through the free volume and voids of the fiber/matrix interface. The electrochemical reaction occurring at the fiber/matrix interface is modeled by the sub-circuit; R_T in parallel with Q_{DL}. R_T is the charge transfer resistance across the interphase and Q_{DL} is the double layer charging of the interphase.

Experimental and simulated EIS data from model fit are shown for selected cases in the figures in the following pages. Parameter estimates from the equivalent circuit analysis and the significance of the observed changes in these parameters are also discussed.

Case 1: Carbon Fiber/Vinylester composite exposed in seawater at RT with no polarization

Figure 3.23 shows the quality of the fitting curve and Table 3.7 shows the equivalent circuit parameters as a function of exposure time at seawater room temperature condition. It can be seen that the model fit is relative good. The simulation data almost exactly matches with the actual modulus and is a good fit to the phase angle. Pore resistance of the composite began at 2.31E+04 and then decreased to 6.09E+03 as the time progress. This illustrates that electrolyte diffused into the composite and water penetrated the pore structure of the matrix. Capacitance (CPE_C) value found to increase as a function of time from 4.78E-06 to 5.58-05 indicate the absorb water. With n (for CPE_C) values fluctuating between 0.3 to 0.8 means that constant phase element are not behaving like an capacitor.

Table 3.7: Circuit element parameters and values as a function of exposure time at seawater RT

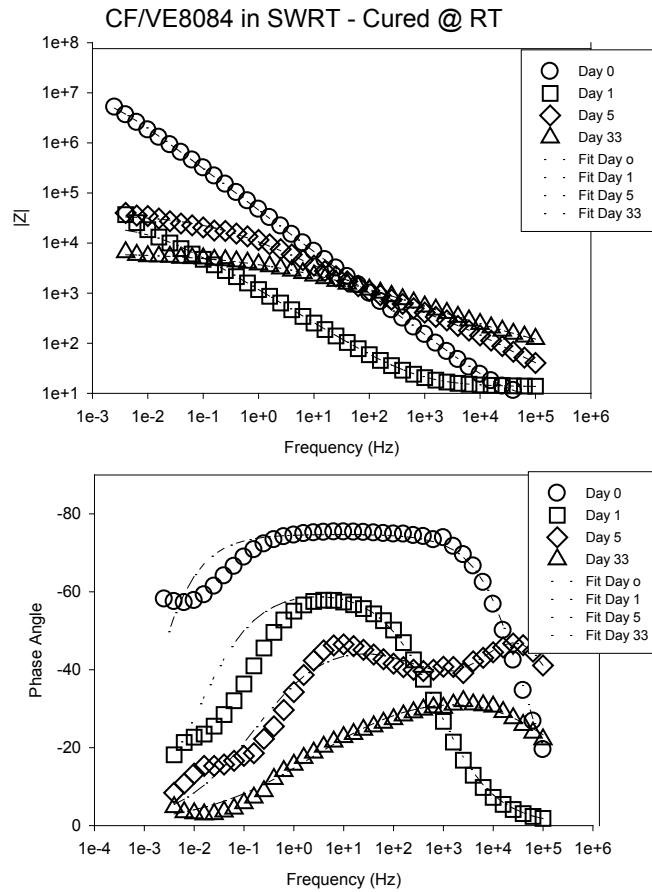| Circuit elements	Day 0	Day 1	Day 5	Day 33
R_S	7.48	1.34E+01	1.66E+01	3.81E+01
CPE_C	4.78E-06	2.39E-04	1.44E-06	5.84E-05
n_{CPE}	8.30E-01	6.78E-01	7.49E-01	3.94E-01
R_{PO}	9.93E+06	2.31E+04	2.89E+02	6.09E+03
Q_{DL}			2.69E-05	
n_{dl}			5.32E-01	
R_T			3.62E+04	

Figure 3.23: Simulated and Actual EIS spectra at seawater RT with no polarization

Case 2: **Carbon fiber/Vinylester composite exposed in seawater at 40C with Stray Current**

Figure 3.24 shows the quality of the fitting curve and Table 3.8 shows the equivalent circuit parameters as a function of exposure time at seawater 40C with stray current condition. The model again provides a good fit. In case of stray current, pore resistance of the composite began at 1.96E+04 and decreased to 3.89E+03 at day 33. This probably was indicative additional water going into the composite due to stray current. Wicking besides diffusion might have taken place as only side was sealed .Capacitance value starts with 3.59E-07 and reached a value of 1.78E-05 at day 33 which indicate the ingress of water into the composite. Double layer capacitance was observed at day 5 starts with a value of 1.77E-03 and slightly increased to 2.21E-03 at day 33. Charge transfer resistance starts with a value of 4.41E+03 and decreased to 2.94E+03 which indicate the interface is offering low resistance as the time progress. At day 5 and day 33, n(dl) value fluctuating between 0.8 and 0.10 means that double layer capacitance is close to a perfect capacitor.

Table 3.8:Circuit element parameters and values as a function of exposure time at seawater 40C with stray current

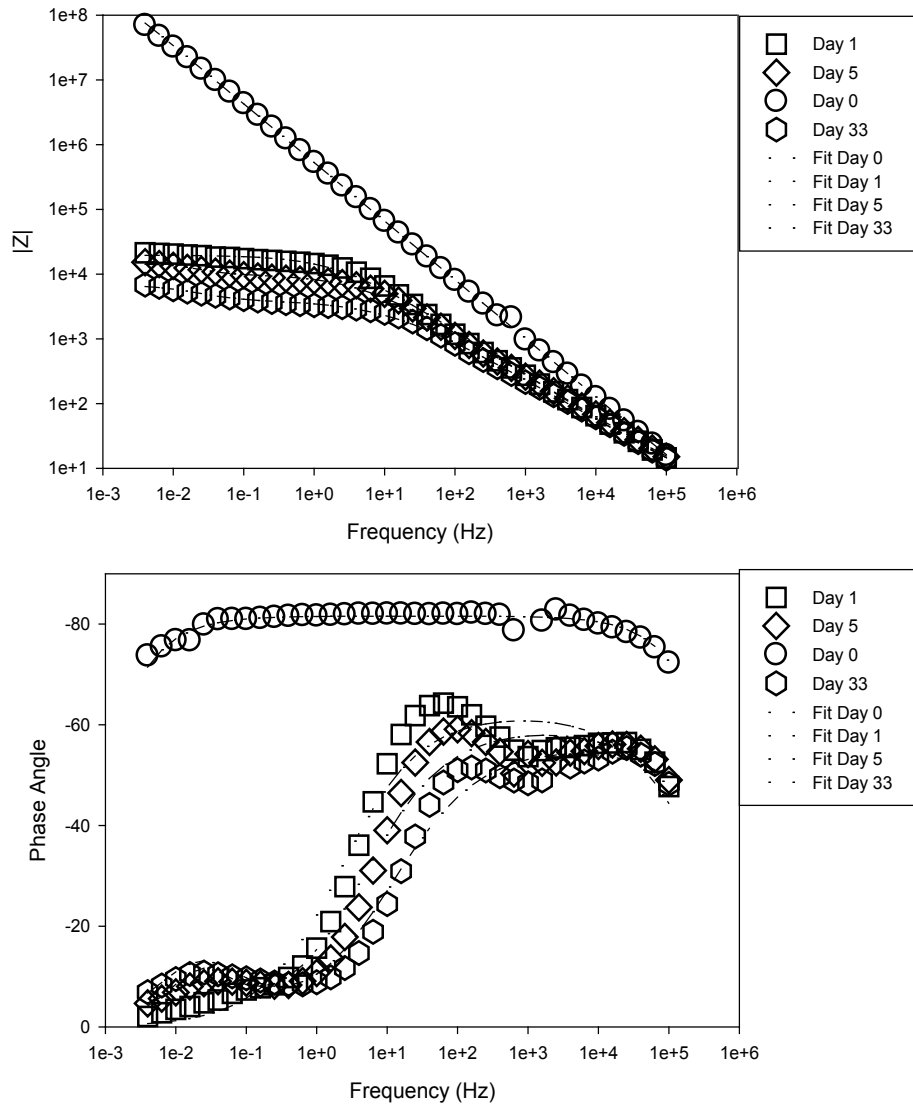| Circuit elements	Day 0	Day 1	Day 5	Day 33
R_S	2.56	5.05	3.75	2.00
CPE_C	3.59E-07	8.41E-06	1.08E-05	1.78E-05
n_{CPE}	9.06E-01	6.93E-01	6.64E-01	6.25E-01
R_{PO}	4.25E+08	1.96E+04	1.00E+04	3.89E+03
Q_{DL}			1.77E-03	2.21E-03
n_{dl}			9.82E-01	8.22E-01
R_T			4.41E+03	2.94E+03

Figure 3.24: Simulated and Actual EIS spectra at seawater 40C with stray current

Case 3: **Carbon Fiber/Vinylester composite exposed in seawater at 40C with galvanic coupling -0.6V**

Figure 3.25 shows the quality of the fitting curve as a function of exposure time at seawater 40C with galvanic coupling (-0.6V) condition. The model provides a good fit with the actual modulus value but the phase angle does not fit is not as good. Table 3.9 lists the change in the equivalent circuit parameters values as a function of exposure time. It can be seen from the table that there was a decrease in pore resistance values. R_P values starts at about 8.37E+03 and decreased to a value of 1.91E+04 indicating seawater penetrated the pore structure. Once seawater reaches the carbon fiber, the applied potential can cause an additional reduction in the pore resistance due to the hydroxyl ions produced by the oxygen reduction reaction. Previous studies by Brown, et al [33] have also shown somewhat similar results, but we did not observed the blistering reported by Brown as our samples were fully immersed in seawater in a large volume and Brown's and others only had a small volume in which pH can increase significantly. According to Brown, the hydroxyl ions subsequently produced a chemical attack on the polymer with possible dissolution of the vinylester matrix. Table 3.9 showed capacitance value starts with 1.76E-06 and increased to a value of 2.33E-05 at day 33. Double layer capacitance (Q_{DL}) was found at day 1 starts with a value of 3.69E-04 and decreased to a value of 9.22E-05. On the other hand, charge transfer resistance (R_T) starts with a value of 6.61E+03 and increased to a value of 1.35E+05 which means they are offering more resistance to transfer charge into the composite interface. This is in good agreement with the double layer capacitance value as the R_T is in parallel with Q_{DL}.

Table 3.9: Circuit element parameters and values as a function of exposure time at Seawater 40C with galvanic coupling-0.6V

Circuit Elements	Day 0	Day 1	Day 5	Day 33
R_S	1.16E-01	2.00	0	0
CPE_C	1.76E-06	5.59E-06	1.00E-05	2.33E-05
n_{CPE}	7.53E-01	6.71E-01	6.22E-01	4.76E-01
R_{PO}	3.04E+05	8.37E+03	2.15E+03	1.91E+04
Q_{DL}		3.69E-04	4.79E-04	9.22E-05
n_{dl}		9.59E-01	7.55E-01	6.88E-01
R_T		6.61E+03	3.46E+03	1.35E+05

Figure 3.25: Simulated and Actual EIS spectra at Seawater 40C with galvanic coupling-0.6V

Case 4: **Carbon Fiber/Vinylester composite exposed in seawater at 40C with Galvanic Coupling –Aluminum anode**

Figure 3.26 shows the quality of the fitting curve as a function of exposure time at seawater 40C with galvanic coupling (Al anode) condition. The model again provides a good fit with the actual modulus value and the phase angle also quite fit very well. Table

3.10 lists the change in the equivalent circuit parameter values as a function of exposure time. The pore resistance value starts with 3.38E-15 at day 1 , increased to a value of 1.051E+03 at day 5 and decreased to a value of 6.31E+02 which indicate the seawater penetrated the pore structure. The most likely mechanism would be hydrolysis of the polymer matrix which is explained for the previous case (galvanic coupling -0.6V). Table 3.10 showed capacitance value starts with a value of 4.77E-07 and increased to a value of6.88E-05. In case of galvanic coupling with aluminum anode, double layer capacitance was also found at day 1 starts with a value of 4.67E-05 and increased to a value of 1.06E-03 at day 33. Charge transfer resistance starts with a value of 1.77E+04 and decreased to a value of 1.92E+03 which indicate charge can transfer into the composite interface. This is also in good agreement with the double layer capacitance value. With n (both n_{CPE} and n_{dl}) values fluctuating between $1 \approx 0.5$ means that constant phase elements are not behave as a perfect capacitor.

Table 3.10: Circuit element parameters and values as a function of exposure time at seawater 40C with Galvanic Coupling-Aluminum anode

Circuit Elements	Day 0	Day 1	Day 5	Day 33
R_S	6.02	4.81	8.43	1.86E+01
CPE_C	4.77E-07	2.29E-04	5.89E-05	6.88E-05
n_{CPE}	8.68E-01	1.99E-01	5.25E-01	5.38E-01
R_{PO}	4.02E+08	3.38E-15	1.05E+03	6.31E+02
Q_{DL}		4.67E-05	1.42E-03	1.06E-03
n_{dl}		5.41E-01	5.61E-01	5.34E-01
R_T		1.77E+04	2.34E+03	1.92E+03

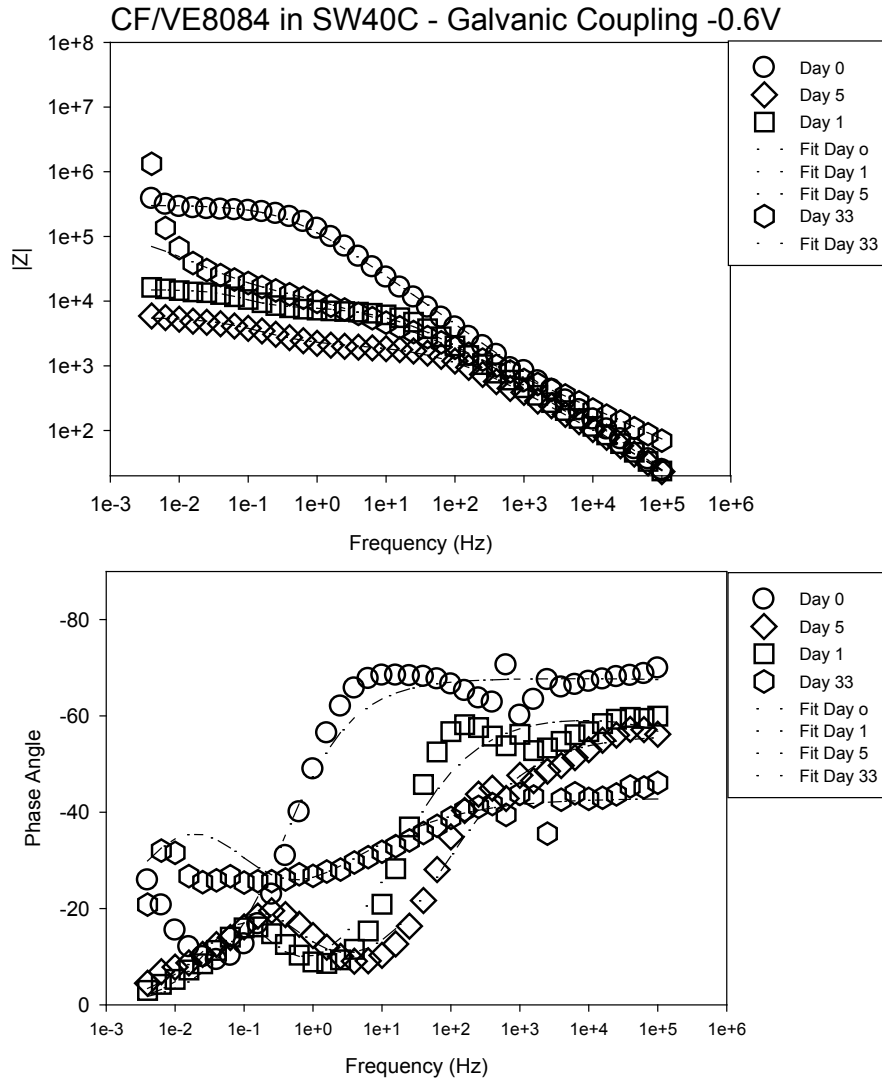CF/VE8084 in SW40C - Galvanic Coupling AL
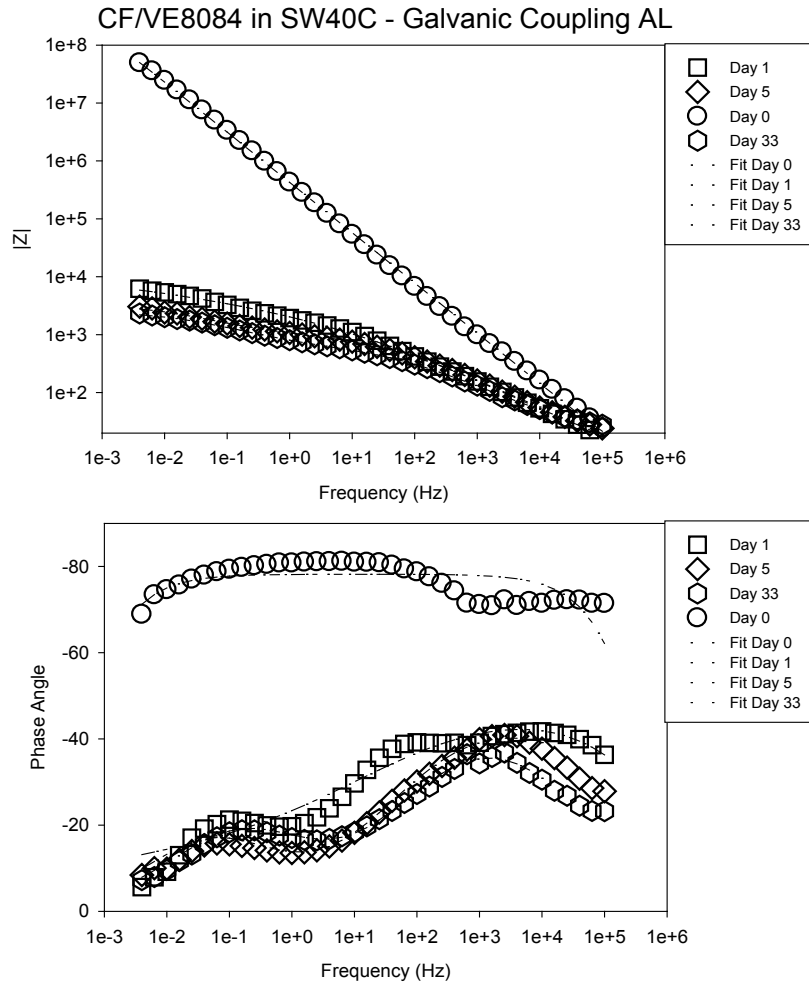
Figure 3.26: Simulated and Actual EIS spectra at Seawater 40C with Galvanic Coupling-Aluminum anode

Case 5: **Carbon Fiber/Vinylester composite exposed in seawater at room temperature -edges sealed with no polarization**

Figure 3.27 shows the quality of the fitting curve and Table 3.11 shows the equivalent circuit parameters as a function of exposure time at seawater room temperature condition with all edges sealed. It can be seen from the figure that the model fits very perfectly. The simulation data almost matches with the actual modulus and is a

very close fit to the phase angle. The equivalent circuit model showed a typical RCR model from day 0 to day 32. Pore resistance starts with a value of 2.63E+19 and decreased to a value of 2.63E+04 at day 32 which is in good agreement with other cases that described previously and what other people [33, 34, 36, 37, 39, 40] have done. Capacitance value starts with 6.96E-04 and increased slightly to 7.47E-04 up to day 5. Moreover, capacitance value decreased slightly to a value of 4.75E-04 at day 32. These findings are almost very similar with the previous studies done by Brown et al [33] and Chris Vinci [32] where the water only penetrates from one face since a small volume is present at all times, whereas all samples tested in here were fully immersed in relatively large seawater tanks.

Table 3.11: Circuit element parameters and values as a function of exposure time at seawater room temperature-Edges sealed with no polarization

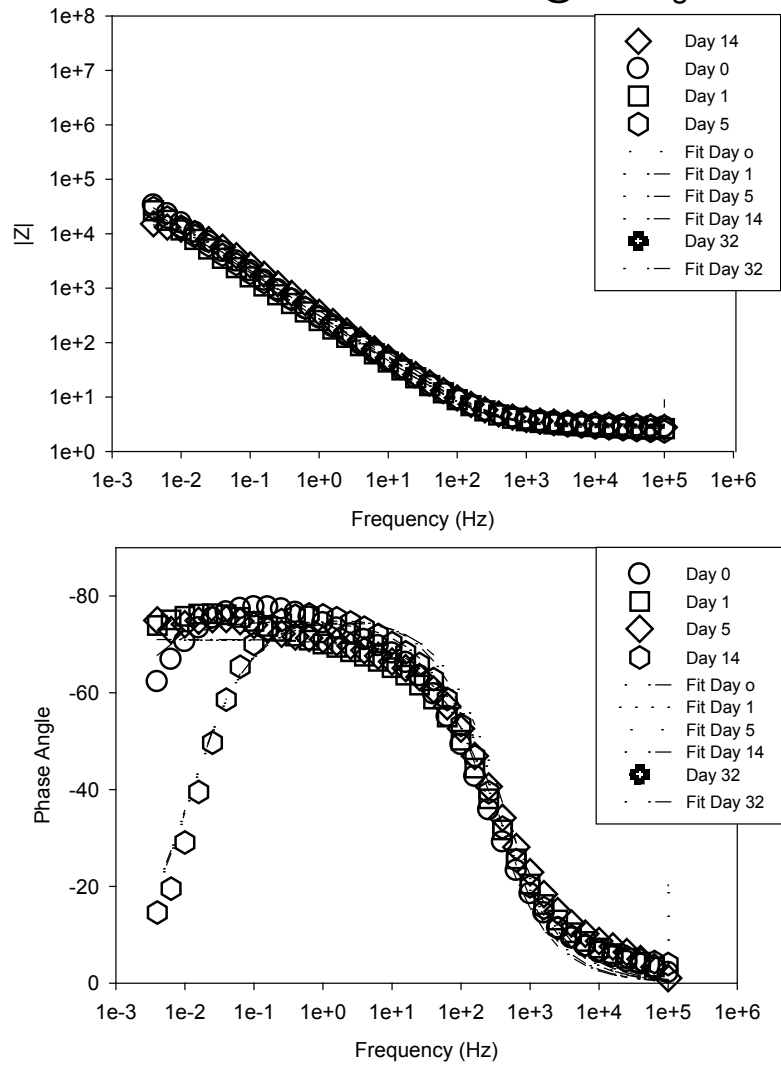| Circuit Elements	Day 0	Day 1	Day 5	Day 32
R_S	3.16	2.82	2.66	2.97
CPE_C	6.96E-04	8.69E-04	7.47E-04	4.75E-04
n_{CPE}	8.33E-01	7.87E-01	7.88E-01	8.42E-01
R_{PO}	2.28E+05	2.63E+19	2.64E+19	1.96E+04

Figure 3.27: Simulated and Actual EIS spectra at Seawater room temperature-Edges sealed with no polarization

3.4.2.2 Correlation between Pore resistance (Rpo) and Flexure strength

Equivalent circuit analysis was performed on EIS spectra ran on day 33 for samples room temperature cured for all different environmental and electrochemical exposures. The Rpo values were selected for comparison vs. the measured flexural strength values. Recall that Rpo is an indicator of the ionic strength of the matrix (hence more concentrated solution in the matrix is present for lower Rpo values). Figure 3.28 shows four plots, the two plots on the left correspond to CF/VE8084 system and the two on the right to CF/VE510A system. The plots on the top row correspond to samples exposed in RT seawater and the plots on the bottom row to samples exposed in seawater at 40C. The label next to each data point indicates what type of electrochemical exposure was applied. For both systems exposed in seawater at room temperature there is an evident linear trend between the two parameters. Except for samples galvanically coupled to an AL anode. A flexural strength reduction was observed for more aggressive electrochemical processes, i.e. OCP (no-electrochemical) < SC (Stray Current) < GC-0.6Vsce. The plots on the bottom row suggest that upon increasing the temperature the trend observed at room temperature is not longer present. The larger Rpo observed on samples polarized at -0.6Vsce in seawater at 40C suggest that calcareous deposits formed at a faster rate and in a uniform layer, preventing some of the ions from reaching the matrix. The sample for 510A system exposed in SW40C and polarized to -0.6 Vsce showed the largest flexural strength of the four conditions shown on the corresponding plot. For 8084 system the sample exposed in SW40C and -0.6Vsce had a flexural strength larger than OCP and SC samples.
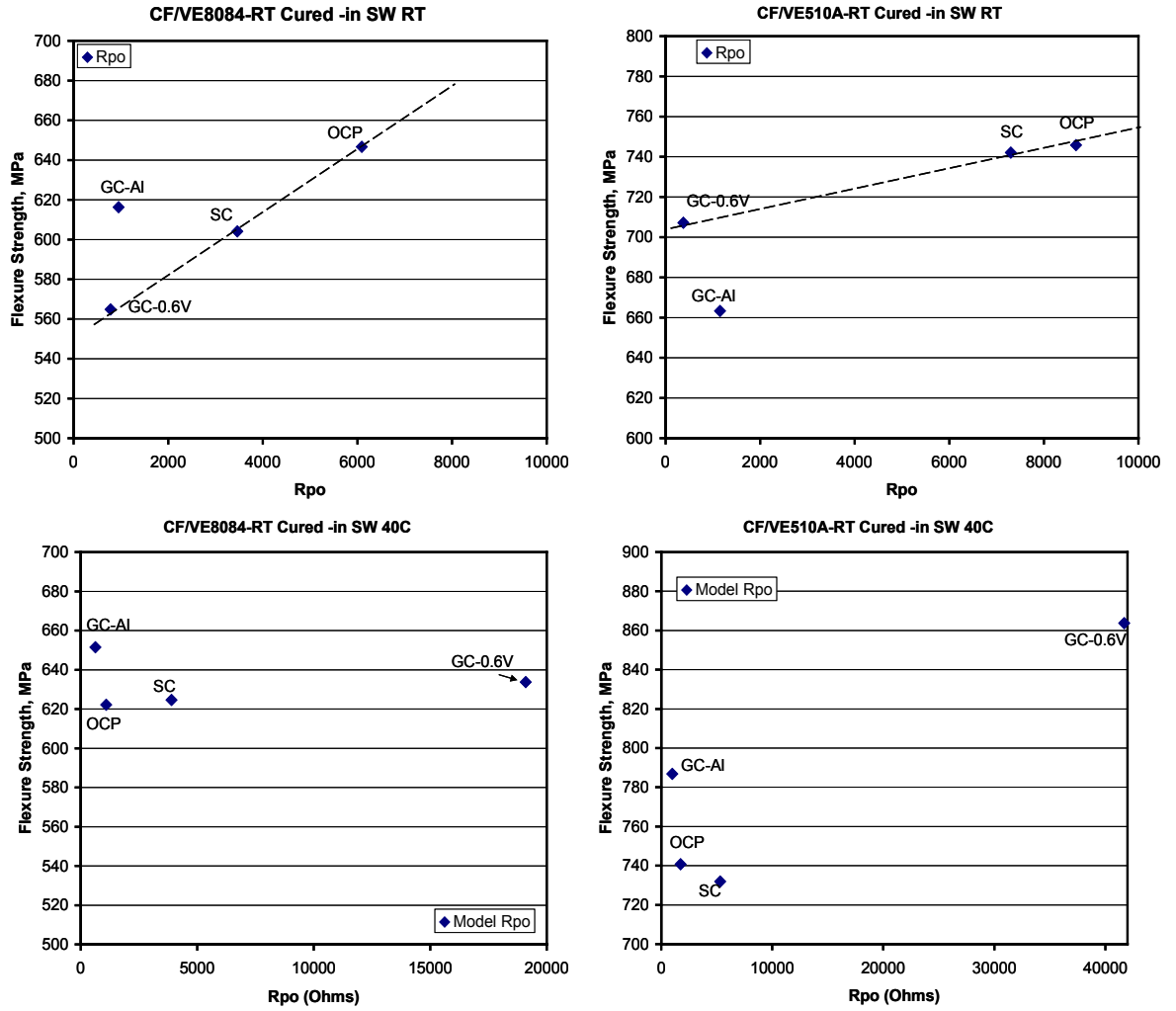
Figure 3.28: Flexural strength vs Rpo comparison

CHAPTER 4：CONCLUSION AND FUTURE WORK

4.1   **Conclusions**

The main objective of this research was to experimentally investigate the degradation of polymer matrix composites exposed in seawater with different environmental and electrochemical interactions. The materials in this project were carbon fiber and two type of vinylester resins currently used in naval applications. The experimental methodology included water absorption measurements of composite specimens by gravimetric analysis, mechanical testing of dry and moisture saturated composite to examine the effect of moisture and electrochemical processes on the integrity of those materials and electrochemical impedance spectroscopy test. The results of this research led to the following conclusion:

- The moisture content of the composite specimens increases with time and temperature for all systems and geometries.
- Higher diffusion rate are observed at higher exposure temperature for seawater immersion, indicating a higher rate of moisture transport. This phenomenon occurred since water diffusion is a thermally activated process [33].
- The diffusion process was found to be Fickian for initial period of exposure only.

- For room temperature cured square specimens, maximum moisture content and diffusion rate are slightly higher for CF/VE 510A than for CF/VE 8084 system for all exposure conditions.

- Exposure to seawater spray and ultraviolet radiation lead to similar moisture absorption behavior than SW at RT exposure.

- Lower rates of water absorption and moisture saturation content were observed for 50° C and 85% relative humidity (RH) humid air exposure.

- The presence of stray currents in SW at RT and 40° C do not affect significantly the moisture absorption for both composite systems.

- Water absorption is more rapid for the flexural specimens compare to the square specimens .Further tests are being pursued to elucidate the reasons for this behavior.

- Reductions in flexural strengths after environmental exposure were evident for all composites. However, these reductions are more significant for the CF/VE8084 system compare to the CF/VE510A system.

- Composite specimens subjected to sprayed seawater and UV radiation experienced the largest reduction in flexural strength, 25% and 16% for CF/VE8084 and CF/VE510A systems respectively.

- The addition of electrochemical processes in the respective environments increases the loss of flexural strength, especially for the VE 8084 resin system. The higher reductions were observed for seawater exposure at room temperature - 0.6.V sce.

- The presence of electrochemical processes enhances the oxygen reduction reaction (ORR) that takes place at the carbon fiber/ liquid interface which degrade the F/M interfaces due to hydrolysis. ORR produces OH^- ions which increase the solution pH, eventually this solution reaches the surfaces of the composite and allows the formation of calcareous deposits, functioning as an additional structural layer.

- The mechanical properties are significantly affected when post-cure is performed on the composite materials. Flexural strength increased by 20% and 16% for CF/VE8084 and CF/VE510A systems at dry conditions after post cured.

- Evident changes of the EIS profiles with exposure time were noted for all conditions investigated.

- Evident differences in the EIS profiles exist when comparing CF/VE 8084 vs. VE 510A same environmental conditions, electrochemical effect at the same age.

- In general there is a reduction of the impedance magnitude with exposure time for all conditions investigated for both composite materials. One possible reason for time dependent decrease in impedance magnitude is moisture absorption and pre-existing defects in the polymer matrix.

- Phase angle for the composite specimens generally shifted toward low frequencies with exposure periods.

- Galvanic coupling with aluminum depresses the phase angle profile significantly after one day of exposure.

- In general, composite specimen showed an increase in matrix capacitance with increase in exposure time. This could be a quantitative indicator of the amount of moisture absorbed by the composite.

- Composite when treated as an electrode showed a continued decrease in pore resistance. This parameter can be determined directly from the EIS plots at relatively high frequency as well as modeling.

4.2 Future Work

- Including neat resin sample in the gravimetric analysis could be useful for comparing water absorbed into the bulk.

- Experimental work is required to determine the degradation of the neat resin properties after moisture saturation.

- Further tests on composite specimens are needed to elucidate the effect of geometry on the moisture diffusion in composites.

- Transverse tensile mechanical testing should be considered because it gives a better indication of the interfacial bond strength.

- To better understand the integrity of fiber/matrix interface, the fracture surface of the failed specimens should be examined using a scanning electron microscope (SEM).

- Further development of EIS for measuring capacitance and gravimetric and capacitance measurements is suggested to calculate the percentage volume of water absorbed at the interface.

APPENDIX

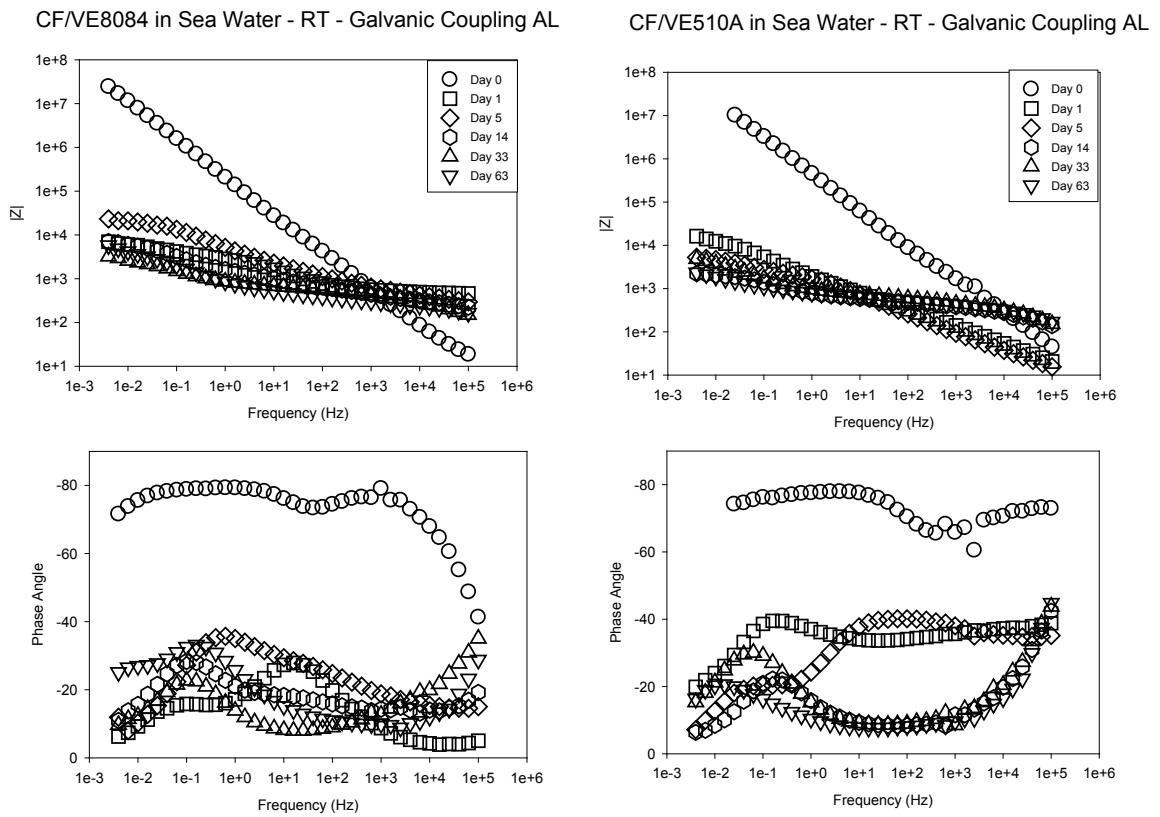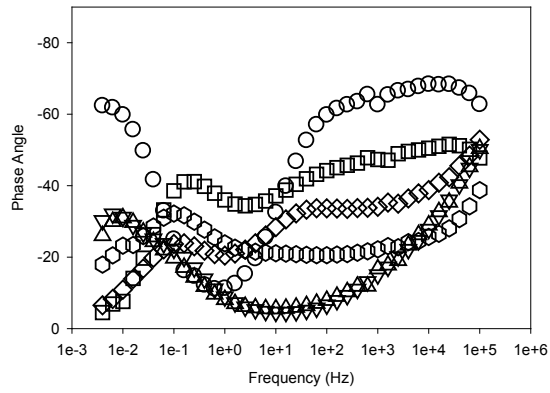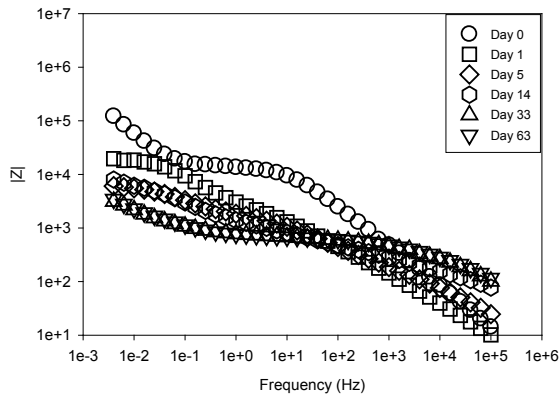**Supplementary Impedance Plots**

Figure A 1.1: Bode magnitude and phase angle for CF/VE composite in SWRT-Galvanic coupling-Aluminum

CF/VE8084 in Sea Water - RT - GC -0.6V
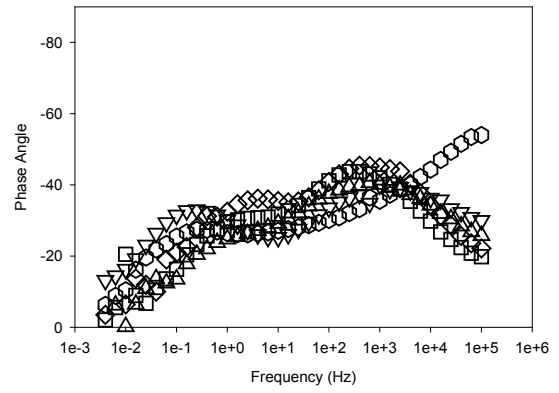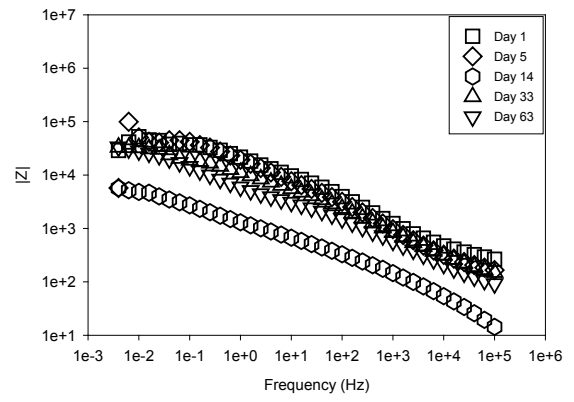
CF/VE510A in Sea Water - RT - GC -0.6V

Figure A 1.2: Bode magnitude and phase angle for CF/VE composite in SWRT-Galvanic coupling-0.6V
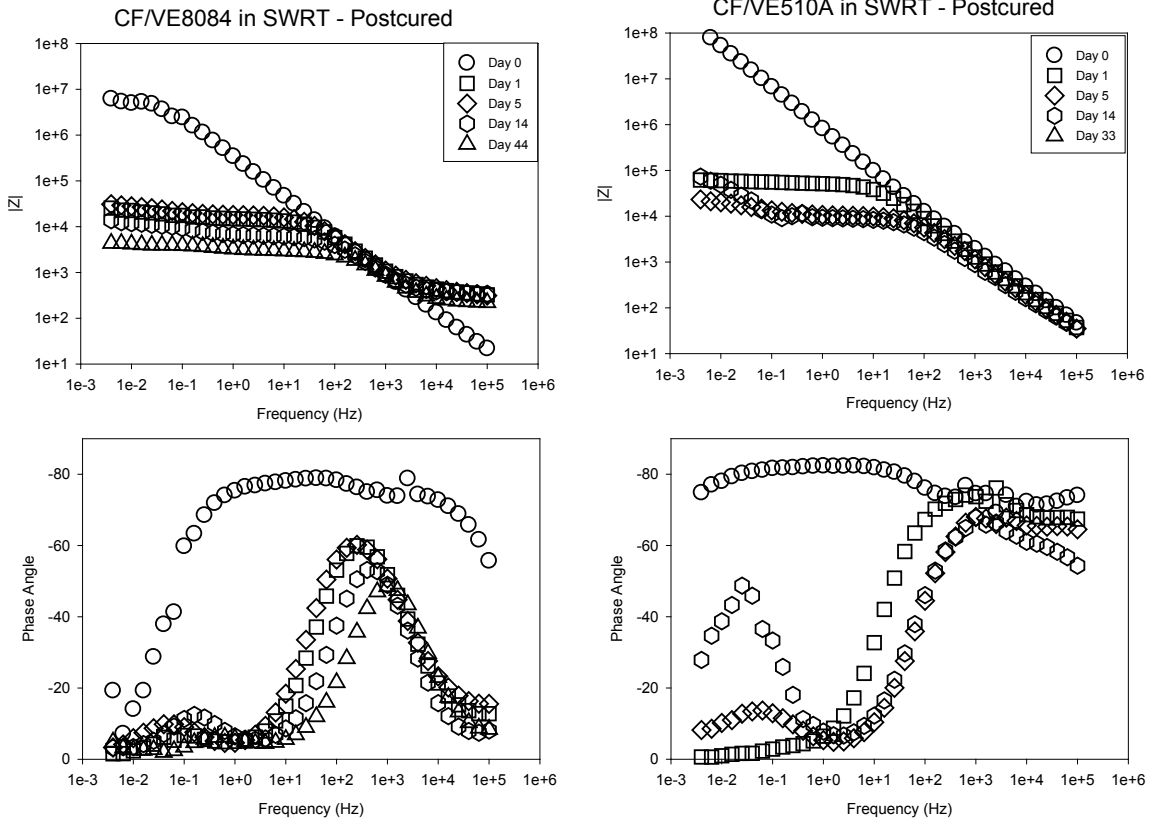
Figure A 1.3: Bode magnitude and phase angle for CF/VE composite in SWRT-Postcured
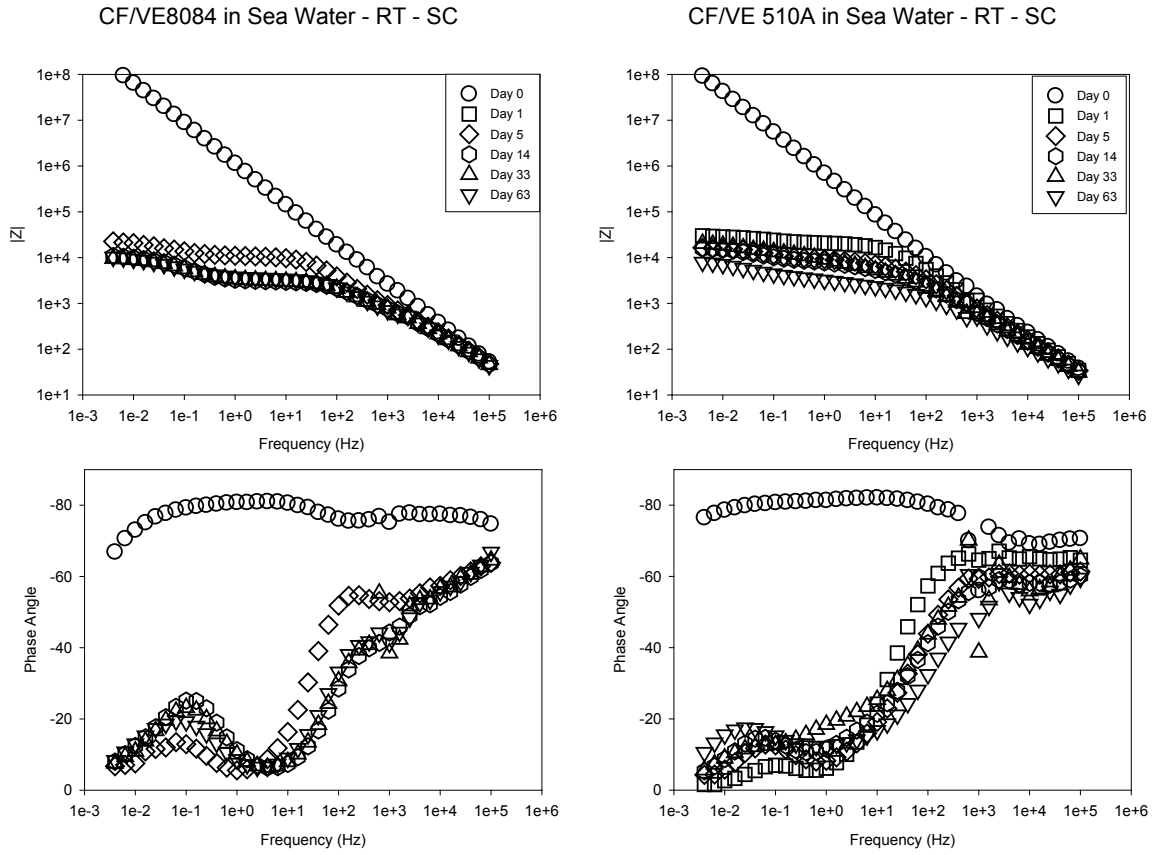
Figure A 1.4: Bode magnitude and phase angle for CF/VE composite in SWRT-Stray current
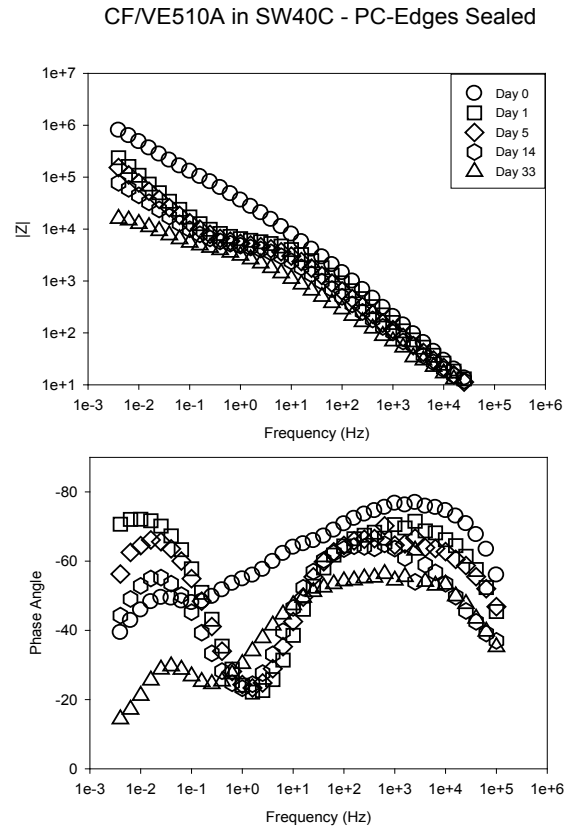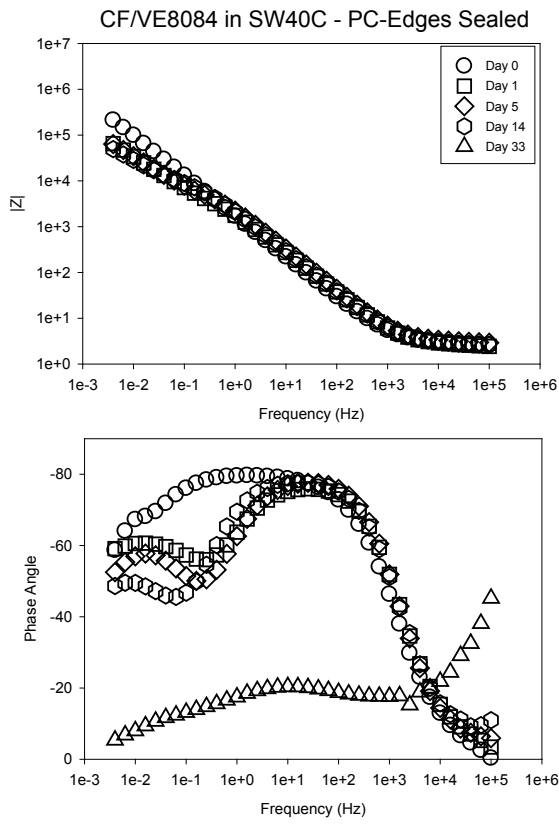
Figure A 1.5: Bode magnitude and phase angle for CF/VE composite in SW40C-Edges sealed

REFERENCES

1. A.P. Mouritz, E. Gellert, P. Burchill, K. Challis, "Review of advanced composite structure for naval ships and submarines" ;Journal of composite structure;2001;53;21-41

2. Naval Technolody.com, "Visby Class Corvettes", Sweden, http://www.naval-technology.com/projects/visby/

3. Naval-Technology.com, "DDG 1000 Zumwalt class-Multimission destroyer advanced technology surface combatants" USA, http://www.naval-technology.com/projects/dd21/

4. Derek Hull, T.W. Clyne, " An introduction to composite materials" , Second Edition, Cambridge University Press, New York, 1996

5. Jean Baptiste Donnet, " Carbon fibers", Third edition, CRC Press, New York, March 19 1998

6. V. Dejke, "Durability and service life prediction of GERP for concrete reinforcement" ;M.Sc, Chalmers University of Technology; Department of Building Materials

7. Vince Kelly's Carbon fiber home page, http://www.geocities.com/vpkelly.geo/

8. A. Kootsookos, A.P. Mouritz, " Seawater durability of glass and carbon polymer composites", Journal of composite science and technology;2004;64;1503-1511

9. Williams, C, "Effect of Water absorption on the room temperature properties of carbon fiber and glass fiber reinforced polymer composites", DTRC-SME, December, 1998

10. G. Sala, " Composite degradation due to fluid absorption" , Journal of composite;2000;31;357-373

11. Lio- Rong- Bao, Albert F. Yee, " Effect of temperature on moisture absorption in a bismaleimide resin and its carbon fiber composites", Journal of polymer scienc,2002; 43;3987-3997

12. T. Nakamura, R.P. Singh, P. Vaddani, " Effect of environmental degradation on flexural failure strength of fiber reinforced composites", Journal of experimental mechanis;2006;46;257-268

13. W.B. Liau, F.P. Tseng, "The effect of long term ultraviolet irradiation on polymer matrix composite", Journal of polymer composite;1998;19;4

14. Chin W, Tihn Nguyen and Khaled Aouadi, "Effect of environmental exposures on fiber reinforced plastic materials used in construction" , Journal of Composite technology and research;Vol.19;205-213,1997

15. Bhavesh G. Kumar, Raman. P. Sing, Toshio Nakamura, " Degradation of carbon fiber reinforced epoxy composite by ultraviolet radiation and condensation", Journal of composite materials;2002;36

16. Kunigal. N. Shivakumar, Gowthaman Swaminathan , Mathew sharpe, " Carbon/vinyl ester composites for enhanced performance in marine applications", journal of reinforced plastics and composites;2006;25;1101

17. E.P. Gellert, D,M, Turely, " Seawater immersion of ageing glass fiber reinforced polymer laminates for marine applications", Journal of composites;1999;part A 30;1259-1265

18. Y.J. Weitsman, M. Elahi, " Effects of fluid on the deformation, strength and durability of polymer composites-an overview", Journal of mechanics of time dependant materials;2000;4;107-126

19. V.M. Karbhari, S, Zhang, " E-glass/Vinyl ester composites in aqueous environments-1:Experimental results", Journal of applied composite materials;2003;10;19-48

20. G.S. Springer, B.A. Sanders, R.W. Rung, "Environmental effects on glass fiber reinforced Polyester and Vinylester Composites", Journal of composite Materials;1980;14;213-232

21. A. Hammami, N. Al-Ghuilani, " Durability and environmental degradation of glass-vinyl ester composites", Journal of Polymer composite;2004;25

22. Lixin Wu, Karen Murphy, Vistasp .M. Karbhari, James. S. Zhang, " Short term effect of sea water on E-glass/vinyl ester composite", Journal of applied polymer science;2002;84;2760-2767

23. A.W. Signor, J.W. Chin, : Effects of Ultraviolet radiation exposure on vinyl ester matrix resins: Chemical and Mechanical characterization", Journal of polymer composite

24. Chi-Hung Shen, George S.Springer, "Moisture absorption and desorption of composite materials" Journal of composite materials; 1976;10;2

25. Chi-Hung Shen, George S. Springer, " Effect of moisture and temperature on the tensile strength of composite materials", Journal of composite materials;1977;11;2

26. C.H. Shen, G.S. Springer, "Environmental effect on composite materials",G.S.Springer; Vol.1-3;Technomic, Lancaster,PA,1981

27. Pomies, F., Carlsson, L.A., Gillespie, J.W. Jr., "Marine Environmental Effects on Polymer Matrix Composites," *Composite Materials: Fatigue and Fracture- Fifth Volume, ASTM STP 1230*, Philadelphia, 1995

28. Geoffrey Pritchard, "Reinforced Plastics Durability", Chapter 3, CRC Press LLC, Boca Raton, 2000

29. M. R. Vanlandingham,R.F. Eduljee, J.W. Gillespie, Jr, " Moisture diffusion in epoxy systems", Journal of applied polymer science;1999;71;787-798

30. G.Z. Xiao, M.E.R. Shanahan, "Water absorption and desorption in an epoxy resin with degradation", Journal of polymer science;1997;35;2659-2670

31. Liang Li, Shu Yong Zhang, Yue Hui Chen, Mojan Liu, Yi Fu Ding, Xiao Wen Luo, Zong Pu, Wei Fang Zhou, Shanjun Li, " Water transportation in epoxy resin", Journal of chemistry of materials;2005;17;839-845

32. Chris J. Vinci, "Carbon fiber/Vinyl ester composite in the marine environment:EIS as a means of determining an effective composite interface"; Thesis; Florida Atlantic University, 2010

33. M.N. Alias, R. Brown, " Damage to composites due to electrochemical processes", Journal of corrosion science;Vol.48;No.5; 1992; 373

34. F.E. Sloan, J.B. Talbot, " Corrosion of Graphite fiber reinforced composites 1-Galvanic coupling damage", Journal of corrosion science;Vol.48;No.10;1992;830

35. Luca Bertolini, Maddalena Carsana, Pietro Pedeferri, " Corrosion behavior of steel in concrete in the presence of stray current", Journal of corrosion science;49;2007;1056-1068

36. S.K. Miriyala, T.J. Rockett, W.C. Tucker and R. Brown, "Blistering of Graphite /Polymer composites Galvanically coupled with metals in seawater", ONR Annual report; 1992

37. F. Bellucci, "Galvanic corrosion between nonmetallic composites and metals 1: effect of metal and of temperature", Journal of corrosion science;Vol.47; No.10; 1991; 808

38. John R. Schully, " Electrochemical Impedance of Organic Coated Steel: Correlation of Impedance Parameters with Long term coating deterioration", Journal of Electrochemical Society ;Vol.136;No.4;1989

39. D. Kaushik, M. N. Alias, R. Brown, " An impedance study of carbon fiber/vinyl ester composite", Journal of corrosion science; Vol.47; No.11; 1991

40. F. Bellucci, "Galvanic corrosion between nonmetallic composites and metals 1: effect of area ratio and environmental degradation", Journal of corrosion science;Vol.47;No.4; 1992; 281

41. M. Kendig, J. Scully, " Basic aspects of electrochemical impedance application for the life prediction of organic coatings on metals" , Journal of corrosion science;Vol.46;No;1;1990

42. J. Qin, R. Brown, S. Ghiorse, R. Shuford, " The effect of carbon fiber type on the electrochemical degradation of carbon fiber polymer composites", Journal of corrosion science

43. ASTM-D5229, " Standard test method for moisture absorption of polymer matrix composites"

44. ASTM-D790, "Standard test method for flexural properties of composites"

45. Gamry Application note, "Basics of electrochemical impedance spectroscopy"

46. ASTM D3171-76, "Standard test method for fiber content of Resin-Matrix composites by matrix digestion" ,Reapproved 1982

47. Felipe A. Ramirez, " Evaluation of water degradation of polymer matrix composites by micromechanical and macro-mechanical tests", Thesis; Florida Atlantic University;2008

48. Frederic Pomies, " Degradation of composite materials in a marine environment", Thesis; Florida Atlantic University

49. Muhammad Umar Farooq, "Degradation of Composite fiber/matrix interface in Marine environment" , Thesis, Florida Atlantic University, 2009

50. Jason J. Chain, Nathan L. Post, John J. Lesko, Scott W. Case, Yin-Nian Lin, Judy S. Ruffle, Paul E. Hess, "Post cure effects on Marine VARTM FRP Composite materials

properties for test and implementation", Journal of Engineering Materials and Technology;128;2006

51. J. Ross. Macdonald, " Impedance spectroscopy", Second Edition, John Wiley & Sons, New York ,2005

52. Herbert H. Uhlig, R. Winston Revie, " Corrosion and corrosion control", 3rd Edition; John Wiley & Sons, New York,1984

53. Andrzej Lasis, " Electrochemical impedance and its application"; Modern aspects of electrochemistry; Vol. 32; 2002; 143-248

54. Basics of Electrochemical Impedance Spectroscopy; Princeton applied research

55. Fraga A.N, Alvarez V.A, Vazquez A, "Relationship between dynamic mechanical properties and water absorption of unsaturated polyester and vinylester glass fiber composites", Journal of Composite Materials, 2003;37

56. Whitney, J.M and Husman, G.E, "Use of the flexure test for determining environmental behavior of fibrous composites", Experimental Mechanics;Vol.4; No.18; 1978

57. Ray A. Grove, "General considerations for continuous fiber composites" , Boeing Commercial Airplane Company

58. Brian W. Smith, " Fractography for continuous fiber composites" , Boeing Commercial Airplane Company

59. Denise M. Aylor, John Murray, "The effect of seawater environment on the galvanic corrosion behavior of graphite/epoxy composite coupled to metals", Report; Carderock Division –Naval Surface-Warfare Center, Bethesda, MD; CDNSWC-SME-92/32-August;1992